

Dynamique et modélisation de la Turbulence



Cours 1-2

sergio.chibbaro@upmc.fr

SB Pope, «Turbulent flows» Cambridge University Press

I am an old man now, and when I die and go to Heaven there are two matters on which I hope enlightenment. One is quantum electro-dynamics and the other is turbulence.

About the former, I am really rather optimistic



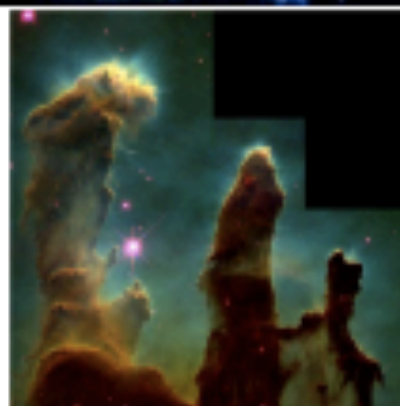
Sir Horace Lamb (1932)

What's Turbulence

- ④ « Turbulence was probably invented by the Devil on the seventh day of Creation when the Good Lord wasn't looking » (P. Bradshaw, 1994)
- ④ « Turbulence is the graveyard of theories » (H.W. Liepmann)
- ④ « ... the absence of a sound theory is one of the most disturbing aspects of the turbulence syndrome » (R.W. Stewart)
- ④ « As a doctorate I proposed to Heisenberg no theme from spectroscopy but the difficult problem of turbulence, in the hope, that if anybody, would solve this problem. However, the problem is until now not solved. » (A. Sommerfeld, 1942)



M100 galaxy 10^{23} m



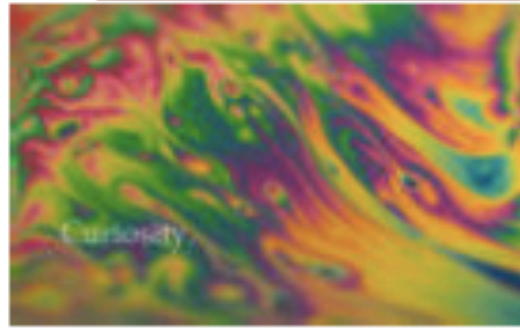
Eagle nebula 10^{18} m



Earth's atmosphere 10^7 m

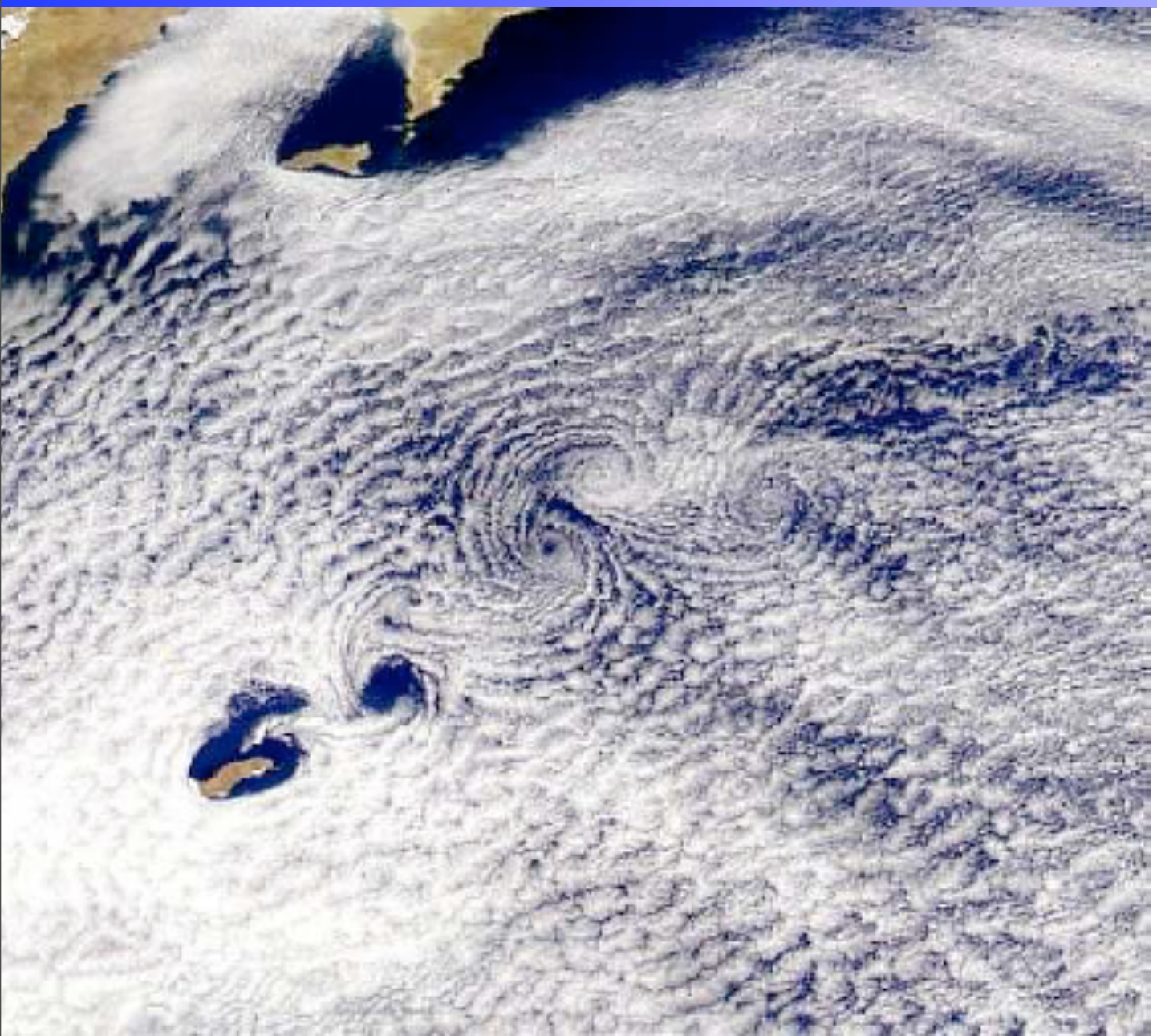


Clouds 10^3 m



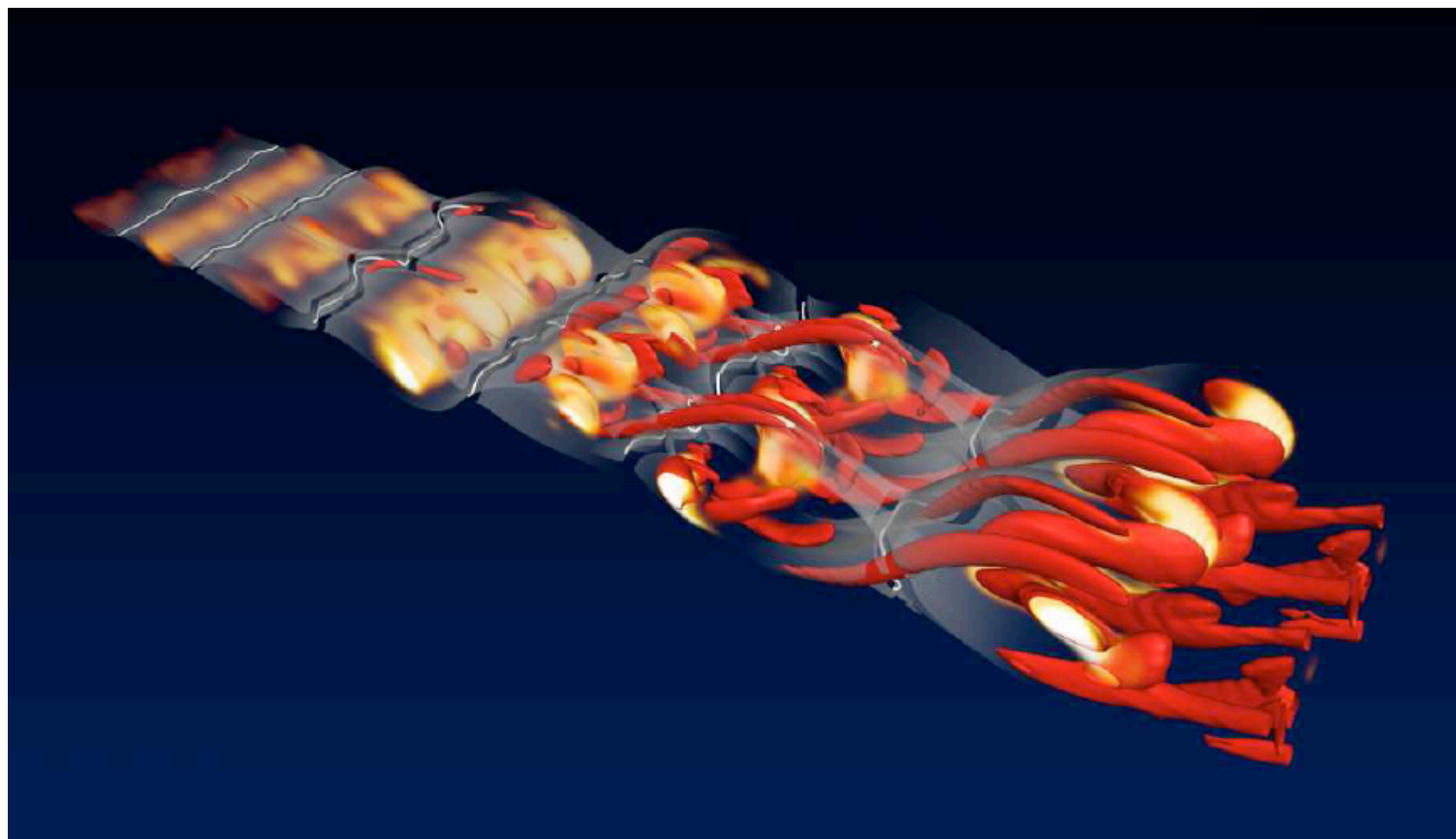
Soap film 10^{-1} m

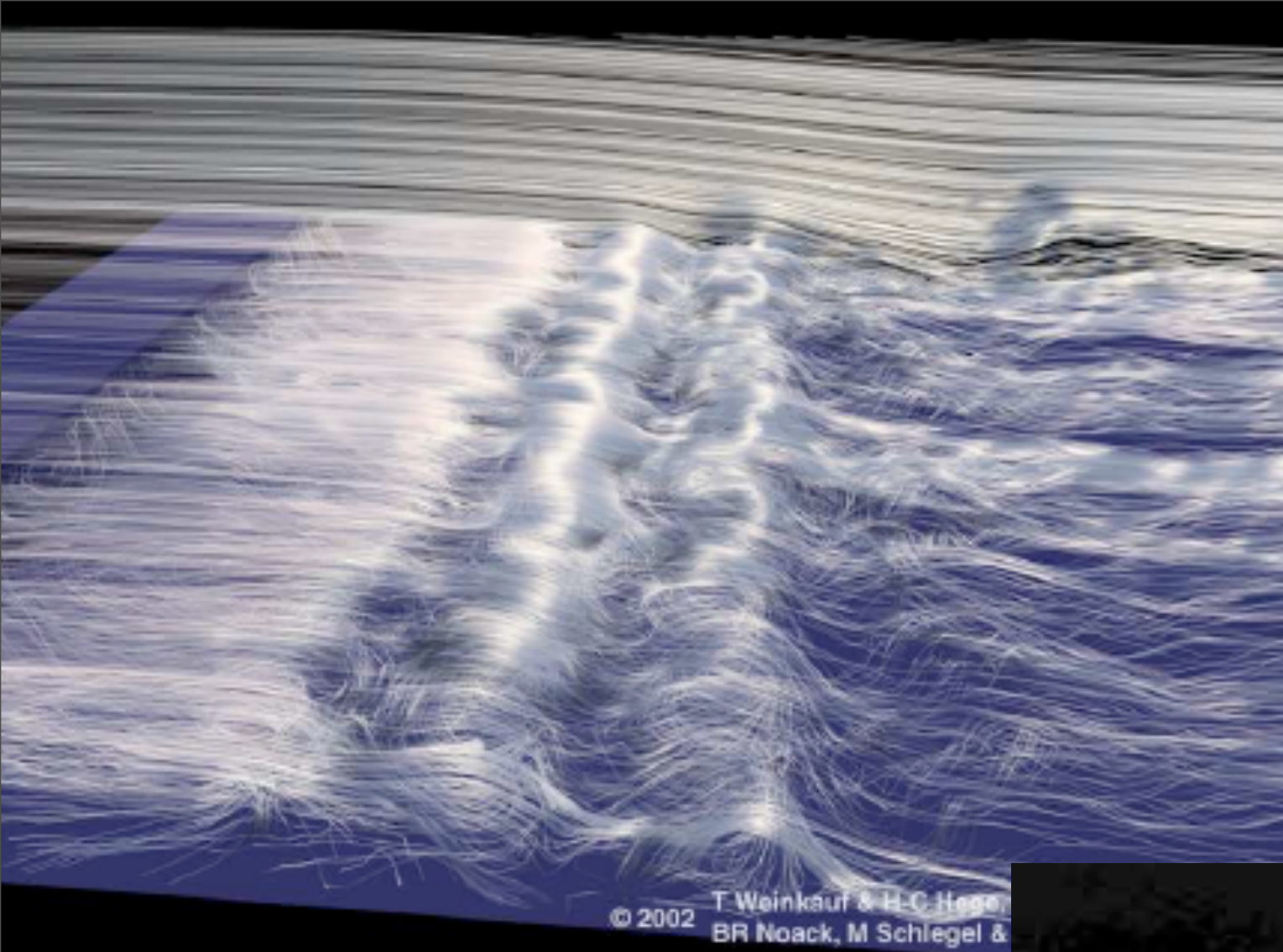
Turbulent flows: illustration and definition





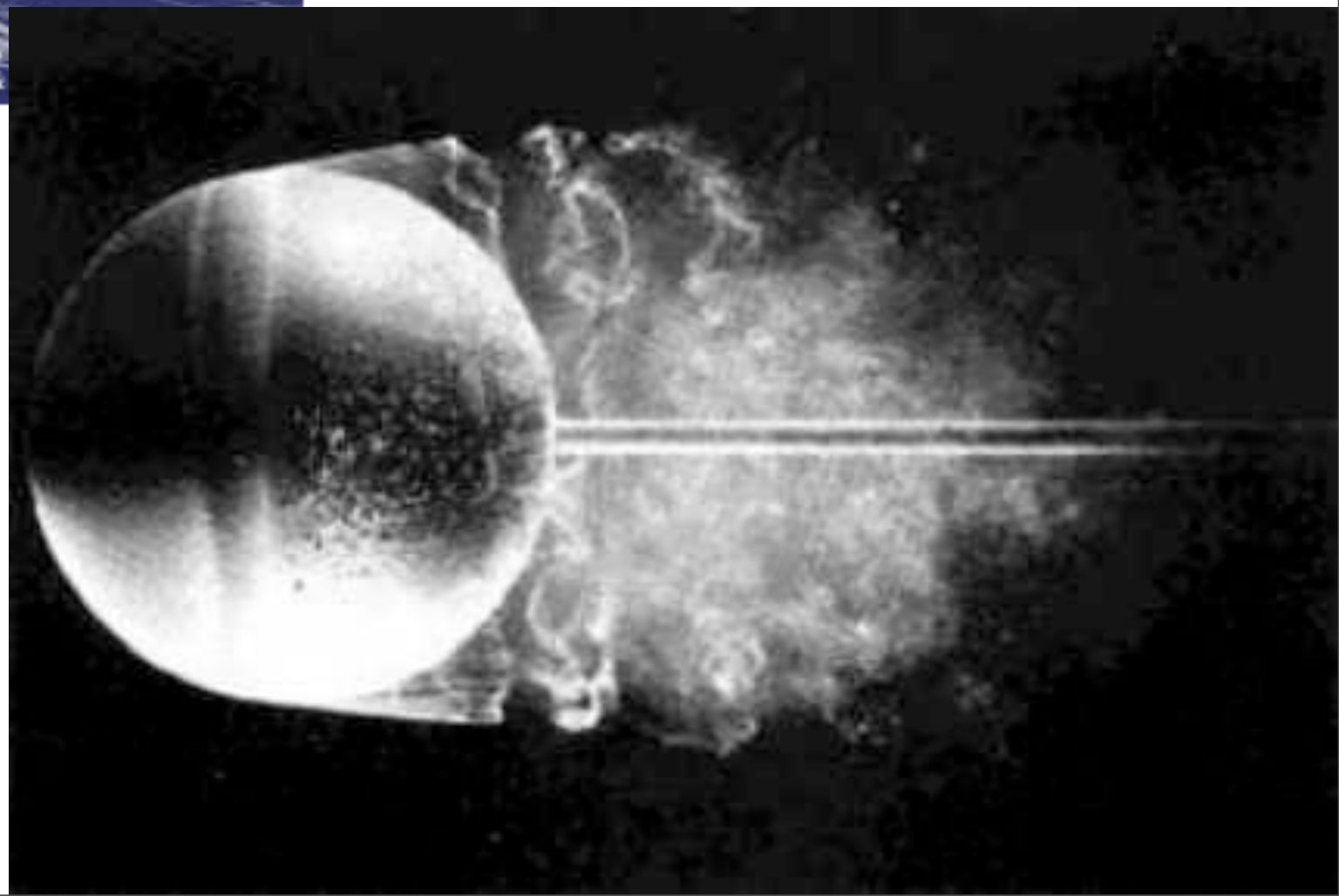
Turbulent mixing layers



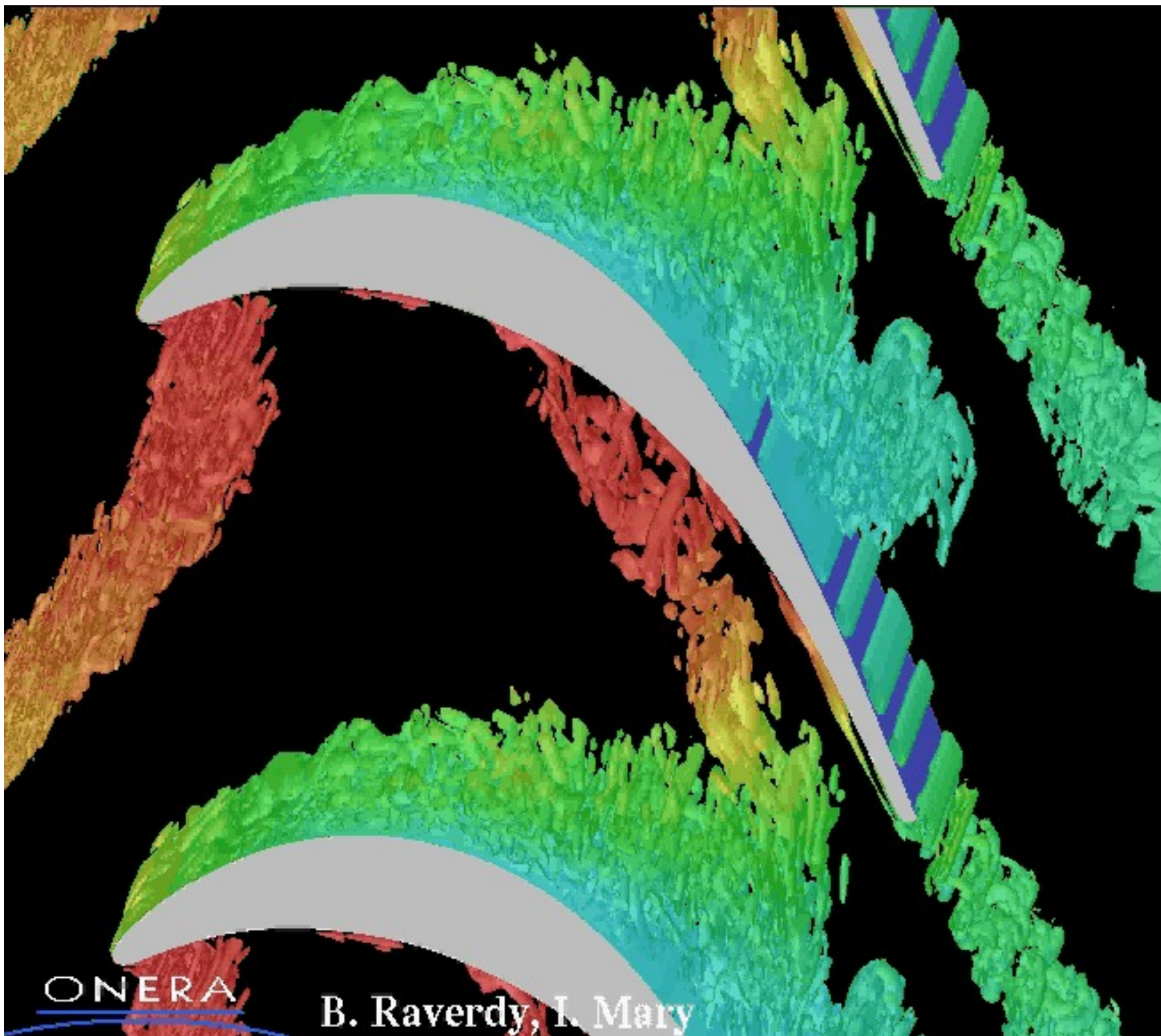


© 2002 T Weinkauf & H-G Hege
BR Noack, M Schlegel &

Backward facing step



Sphere wake



ONERA

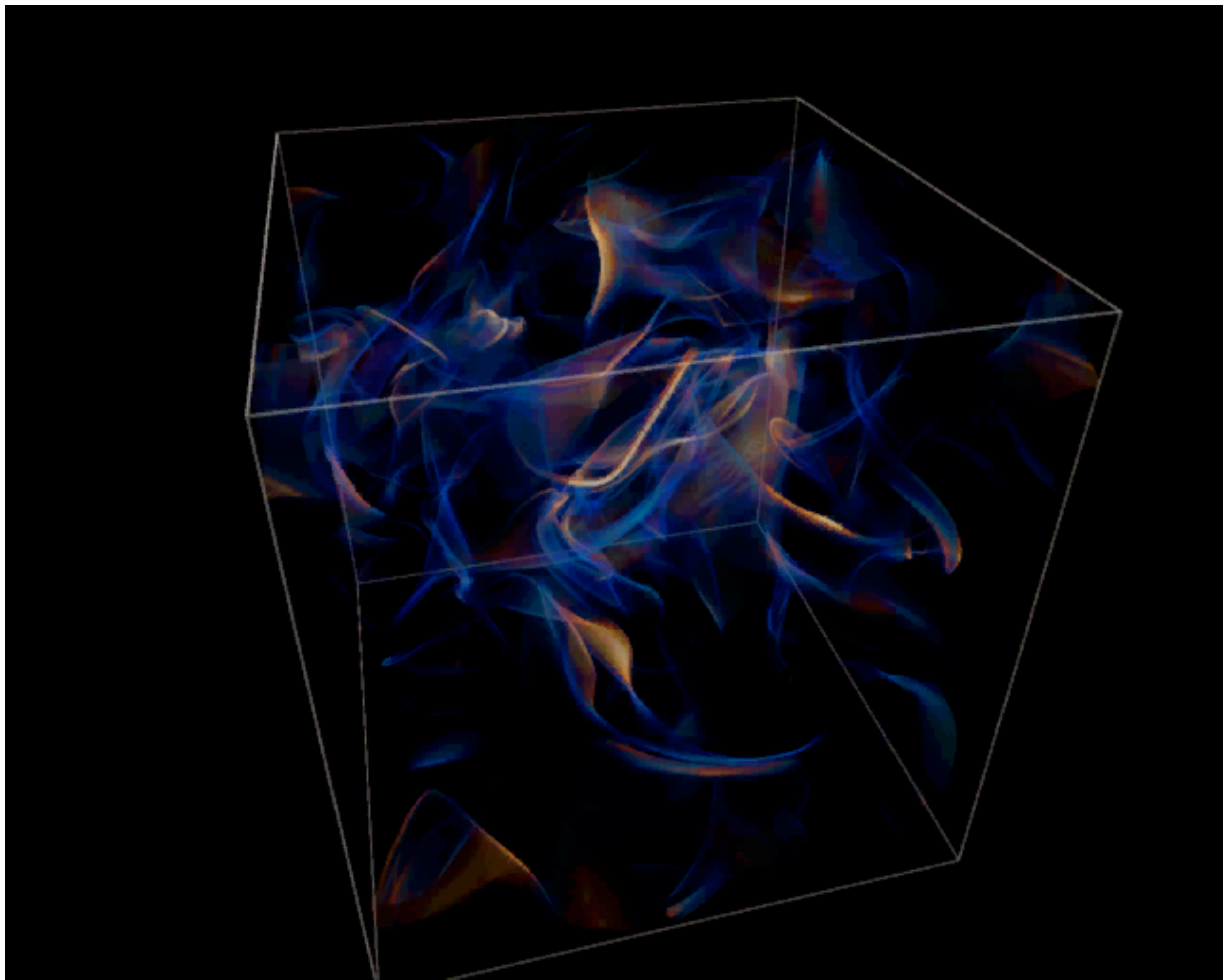
B. Raverdy, I. Mary

Model A

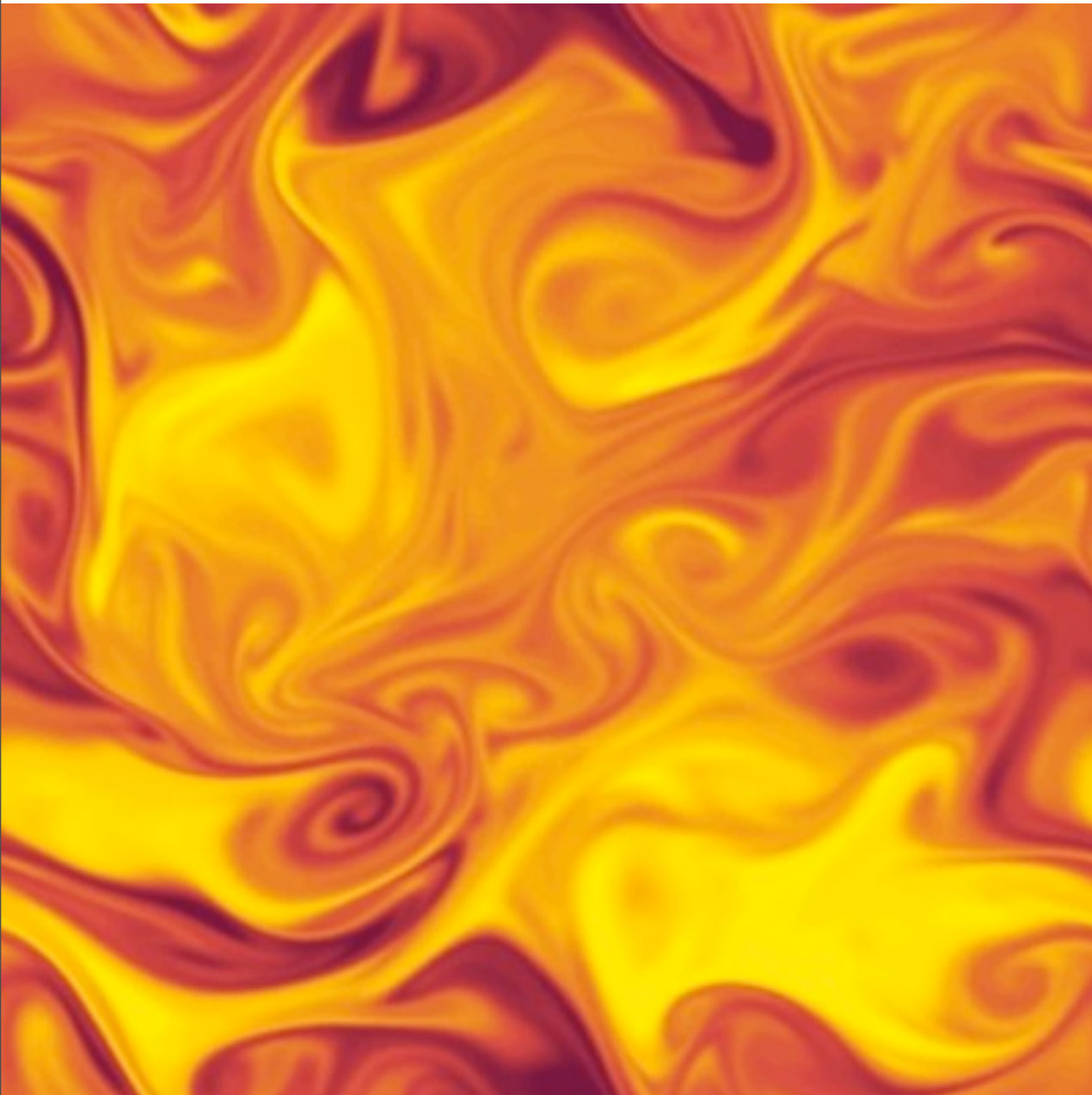


Sports Car



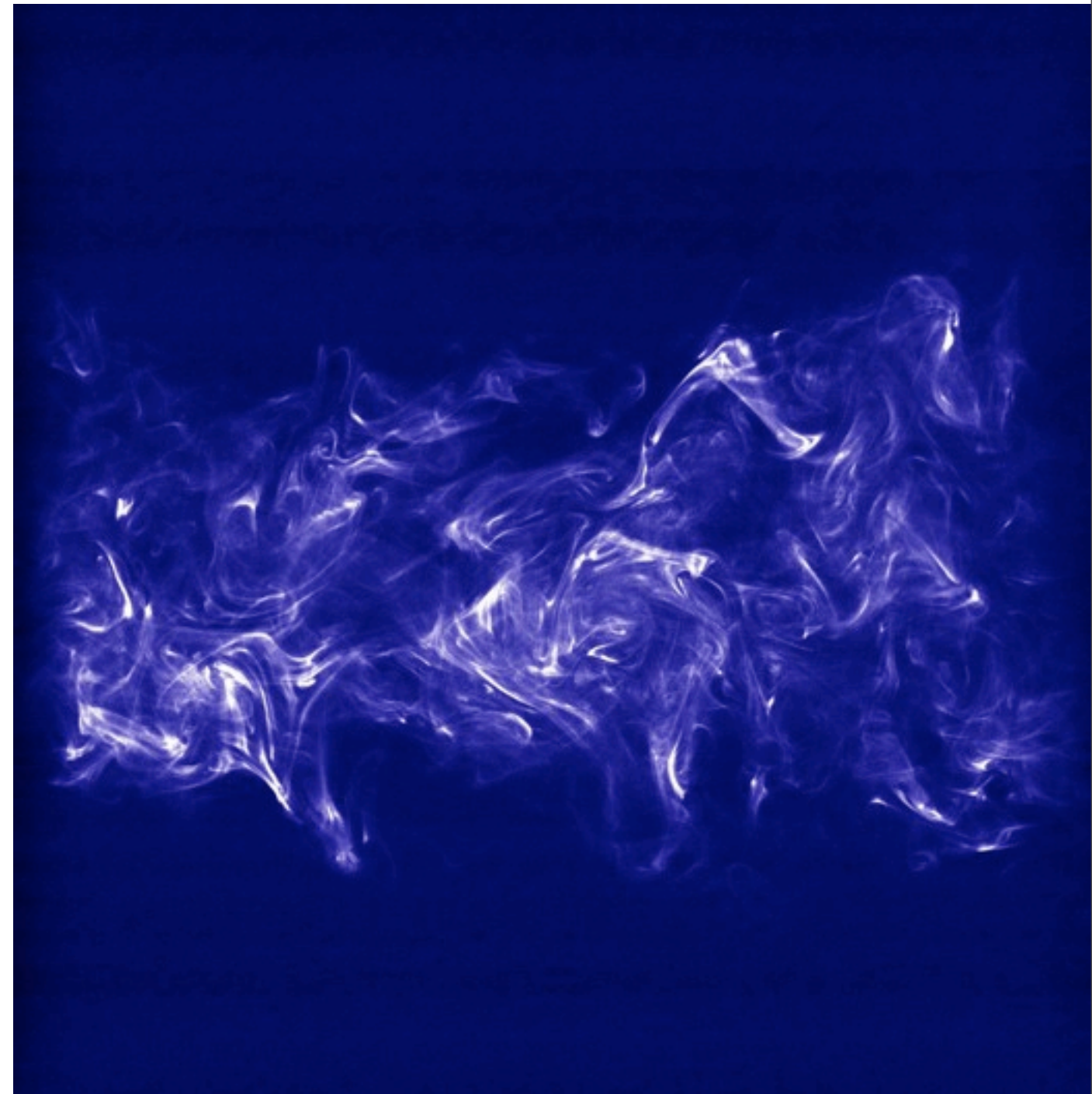


Turbulence & scalar transport



Isotropic turbulence

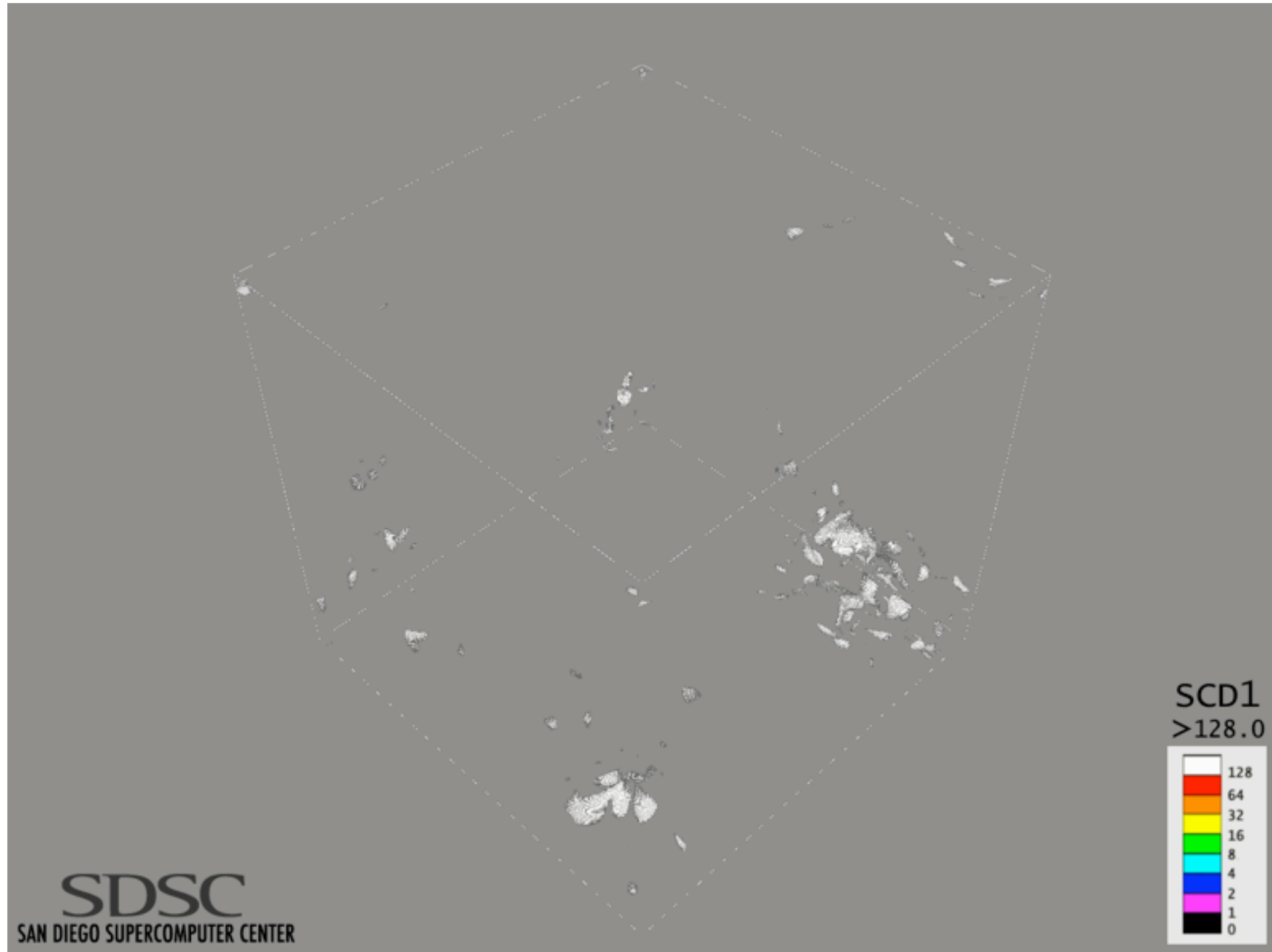
Turbulent jet



Turbulent kinetic energy

dissipation

Turbulent kinetic energy dissipation

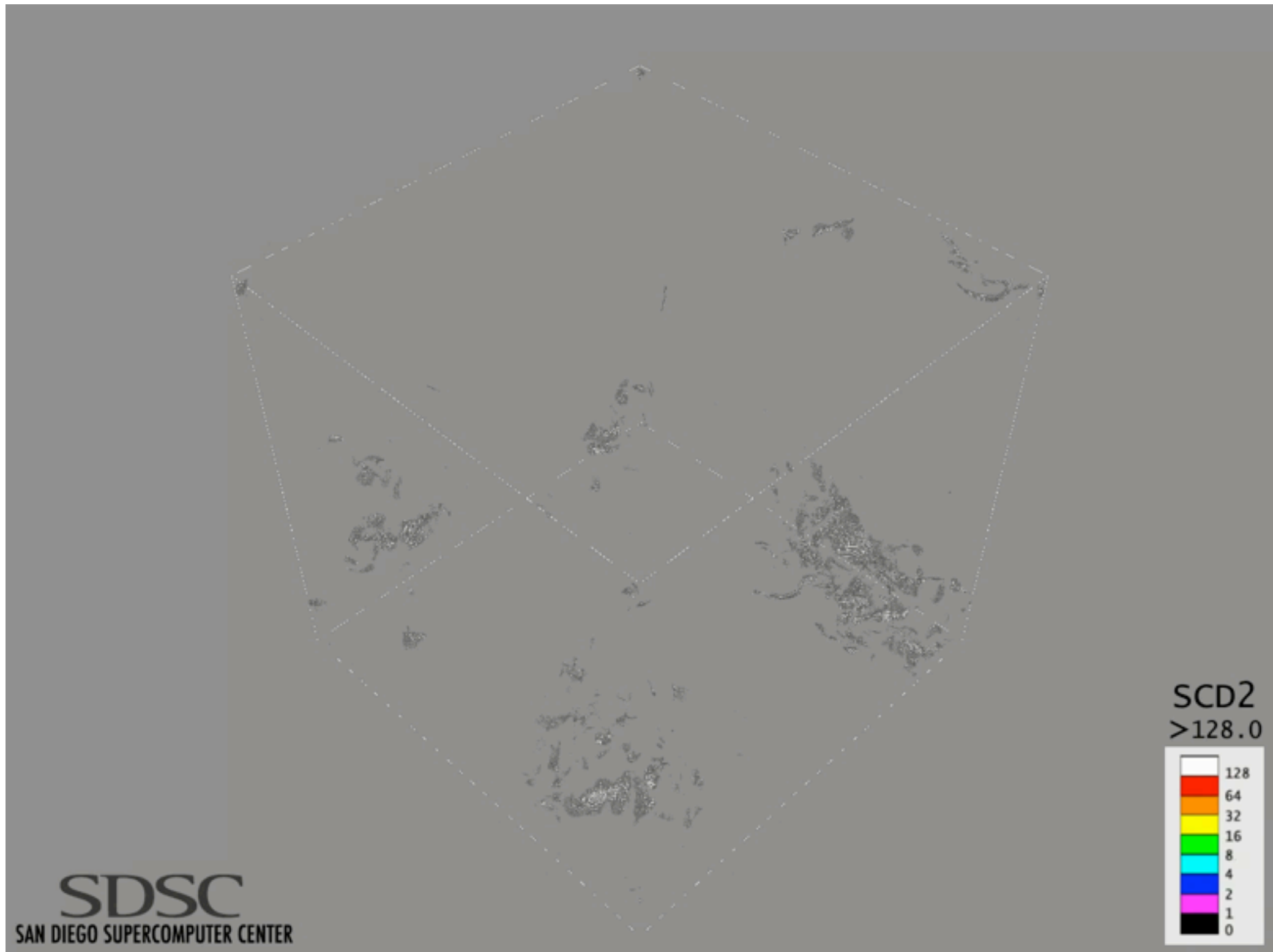


Turbulent kinetic energy

dissipation

Scalar dissipation, $Sc = 4$

Scalar dissipation, Sc = 4



Scalar dissipation, $Sc = 4$

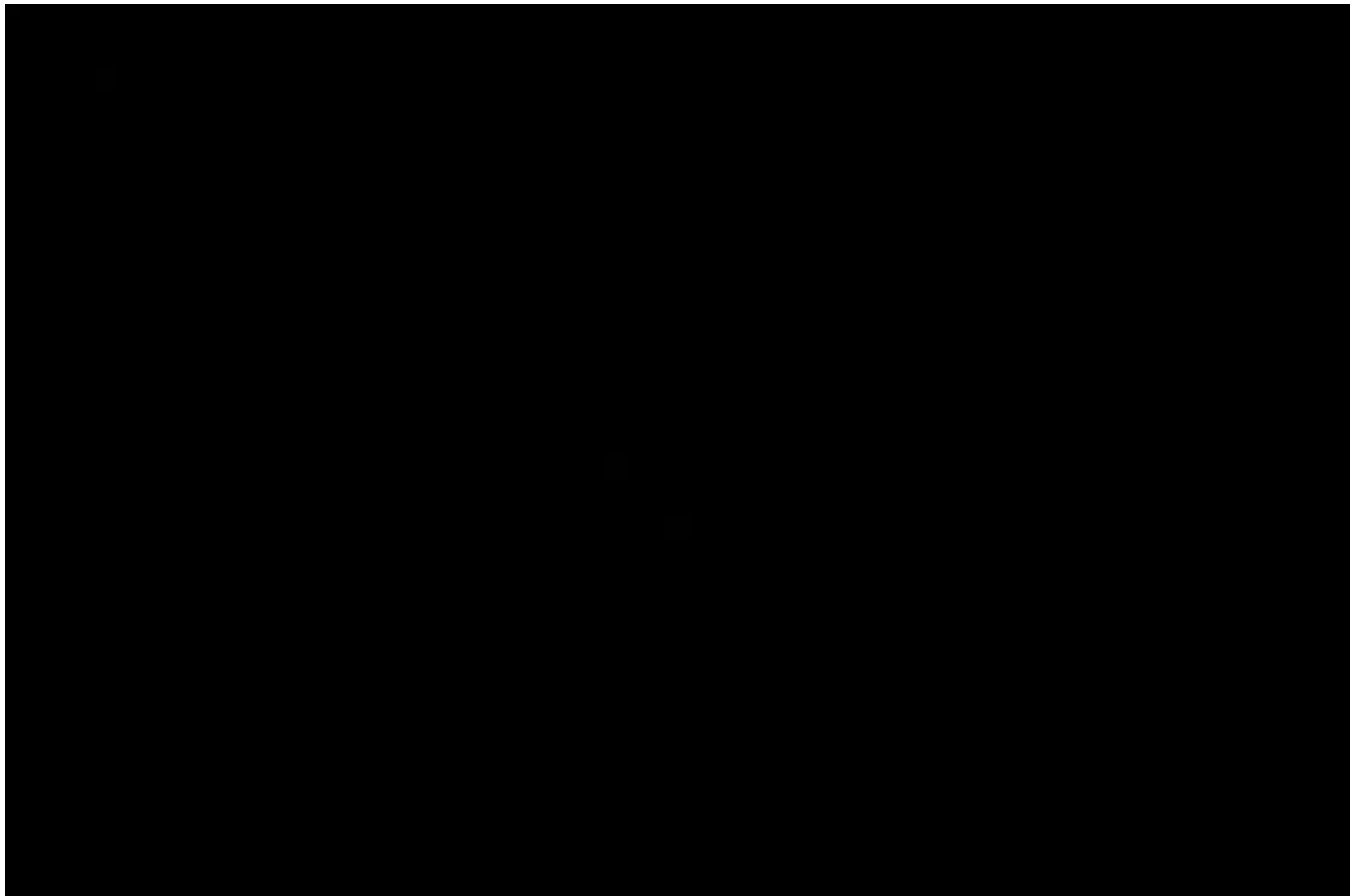
Scalar dissipation, Sc = 64

Scalar dissipation, Sc = 64



Scalar dissipation, Sc = 64

What is a turbulent flow ?



Turbulence and predictions

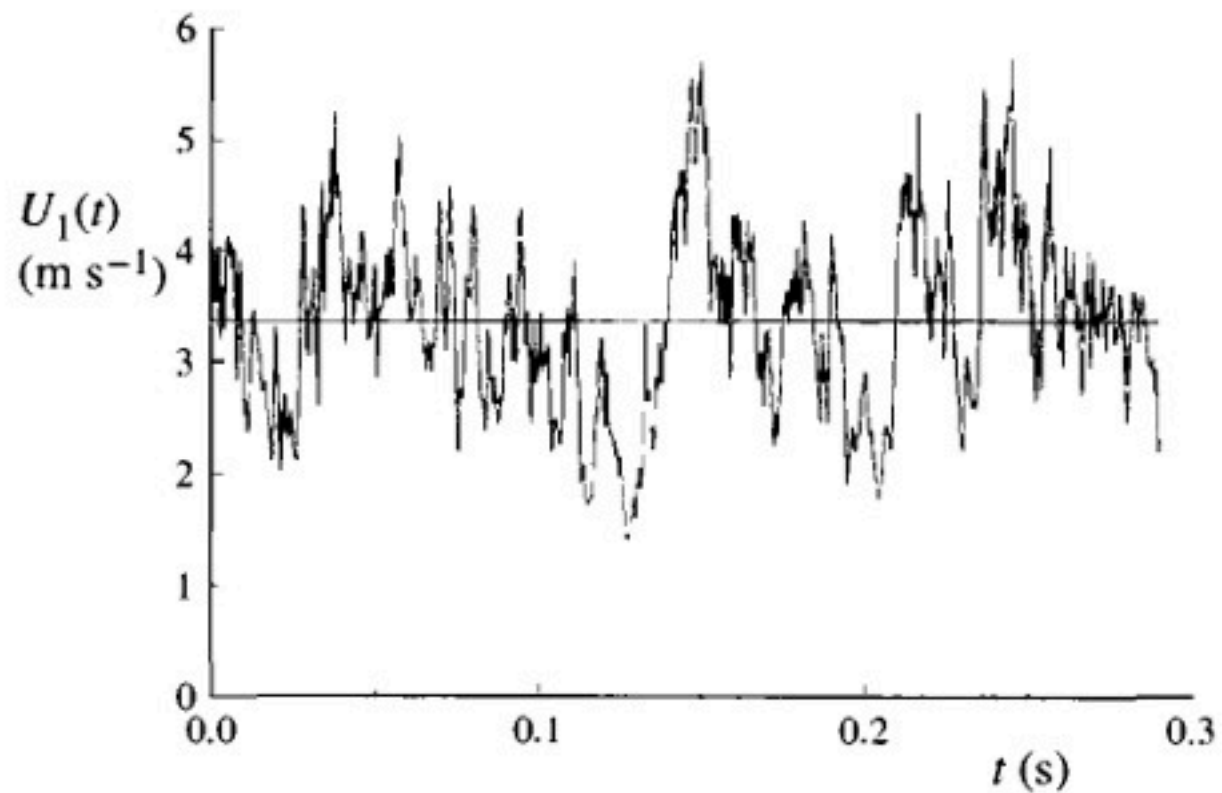


Fig. 1.3. The time history of the axial component of velocity $U_1(t)$ on the centerline of a turbulent jet. From the experiment of Tong and Warhaft (1995).

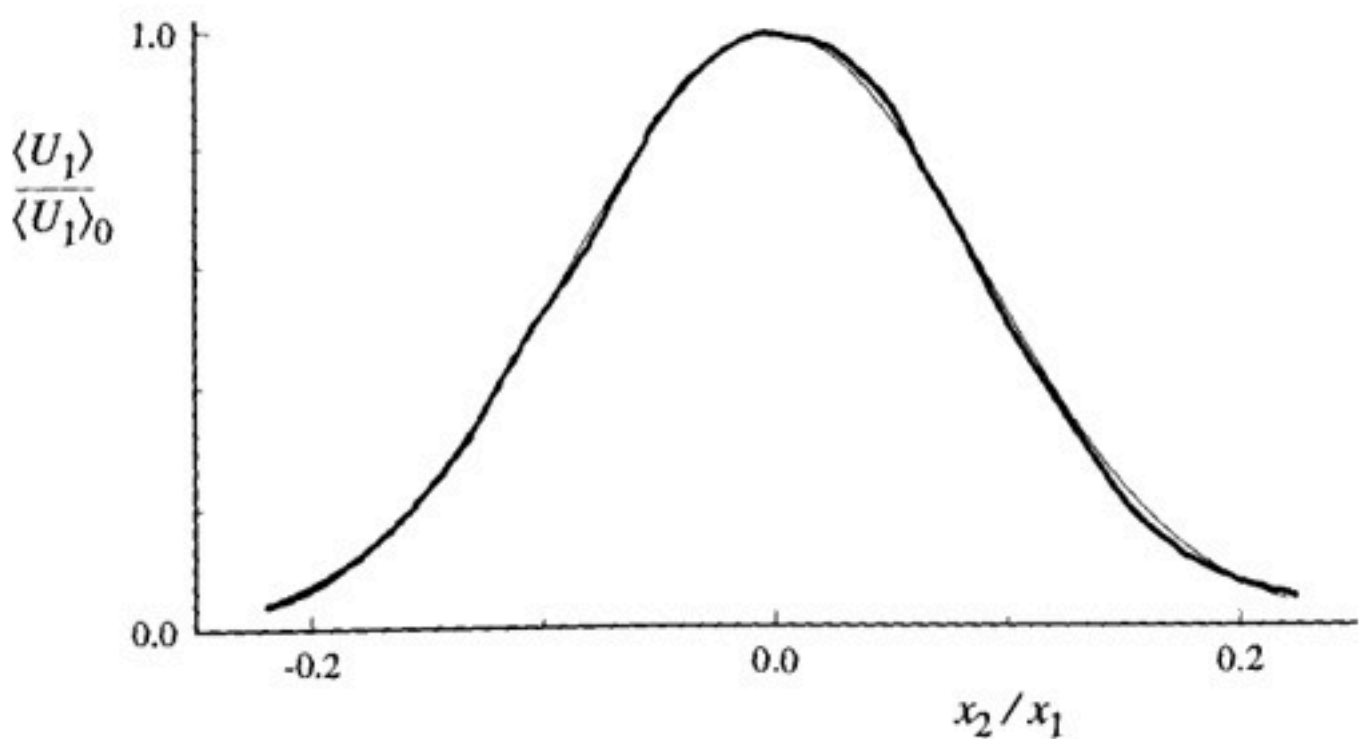


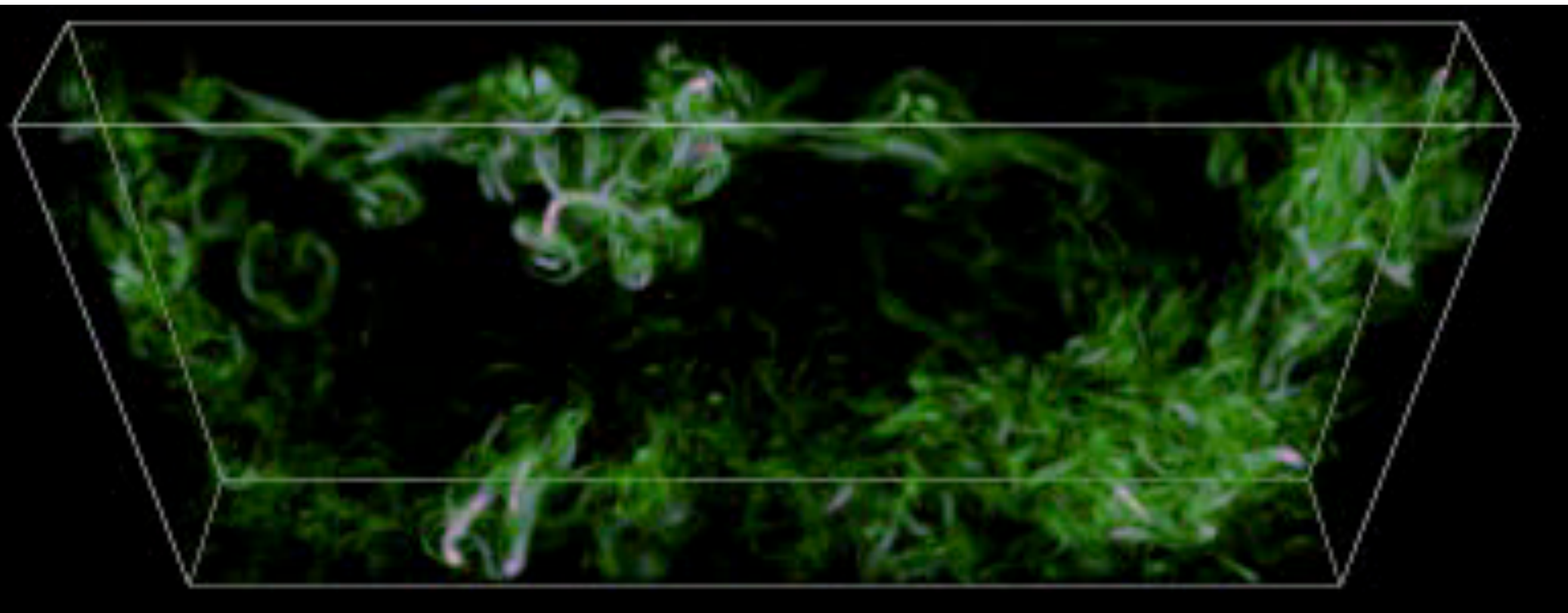
Fig. 1.4. The mean axial velocity profile in a turbulent jet. The mean velocity $\langle U_1 \rangle$ is normalized by its value on the centerline, $\langle U_1 \rangle_0$; and the cross-stream (radial) coordinate x_2 is normalized by the distance from the nozzle x_1 . The Reynolds number is 95,500. Adapted from Hussein, Capp, and George (1994).

Wave Turbulence

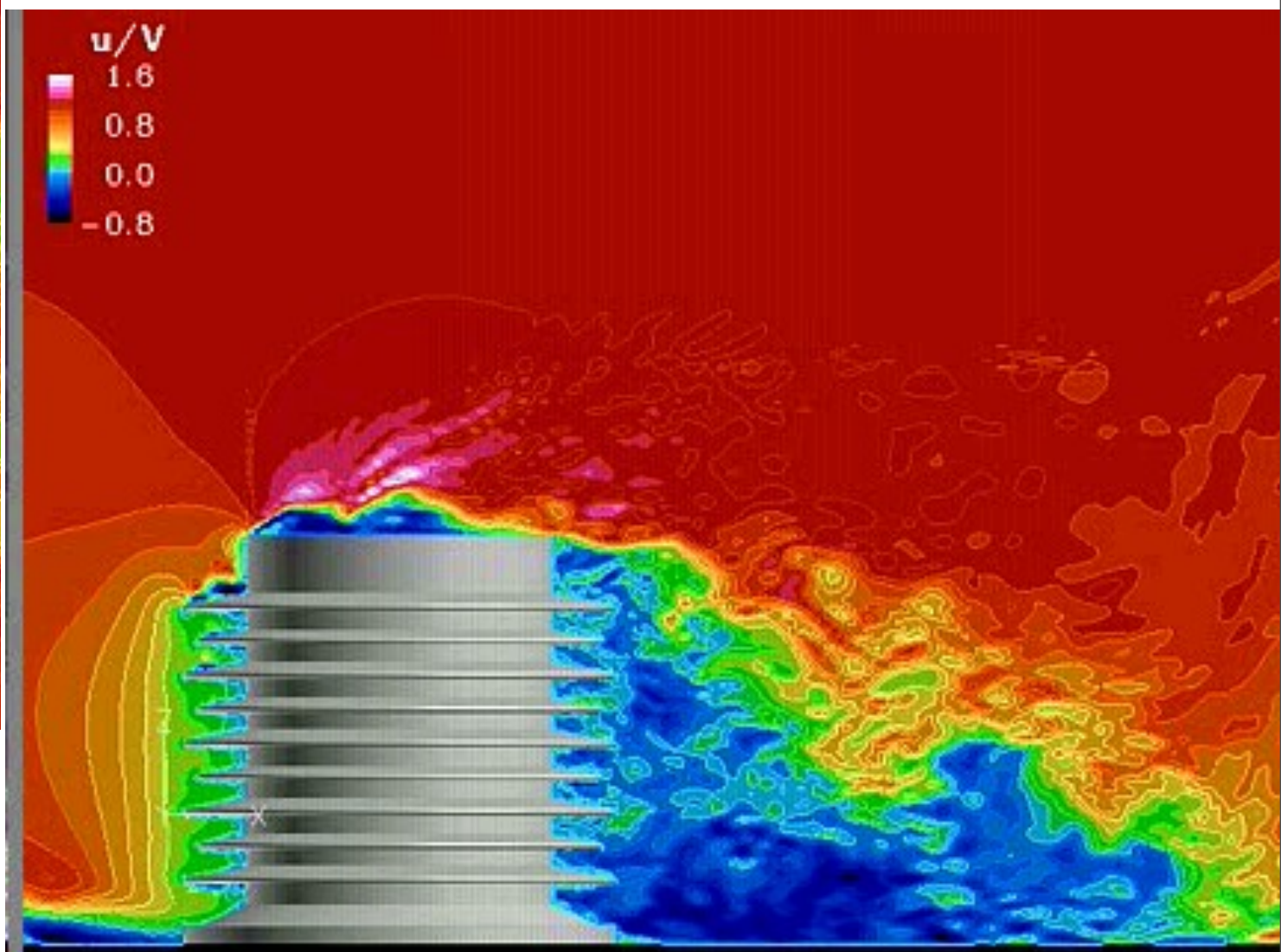
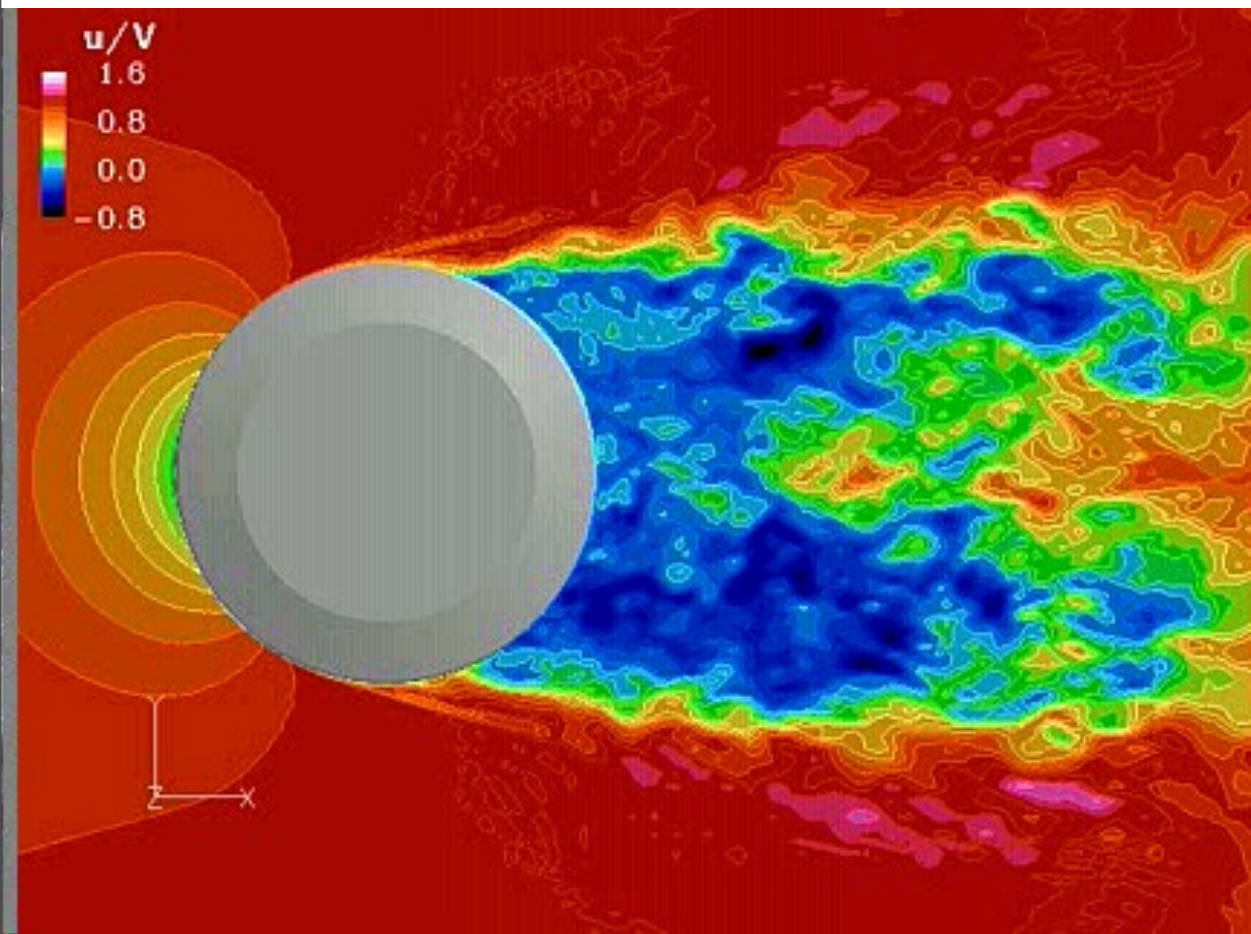


Natural convection

Natural convection



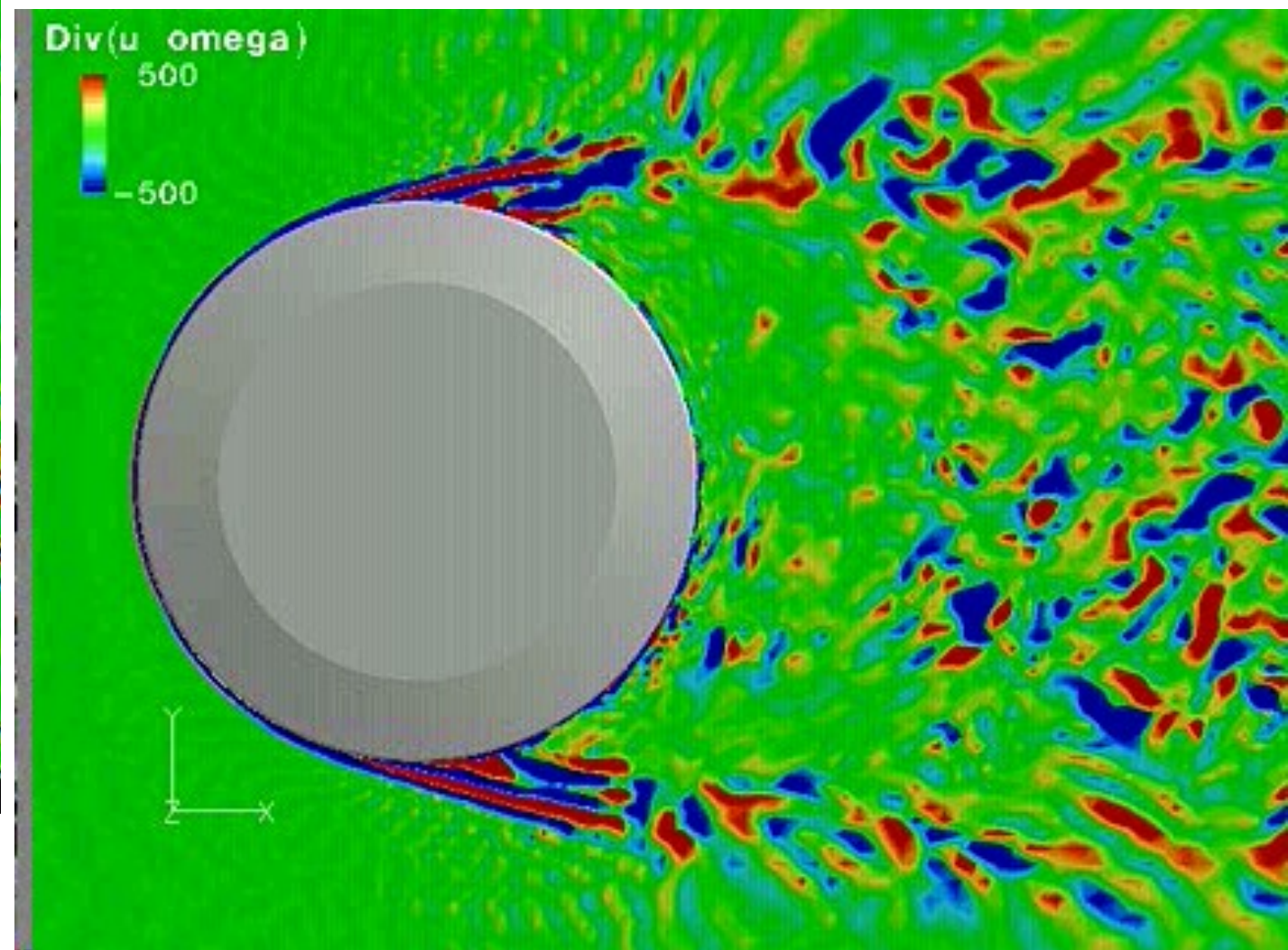
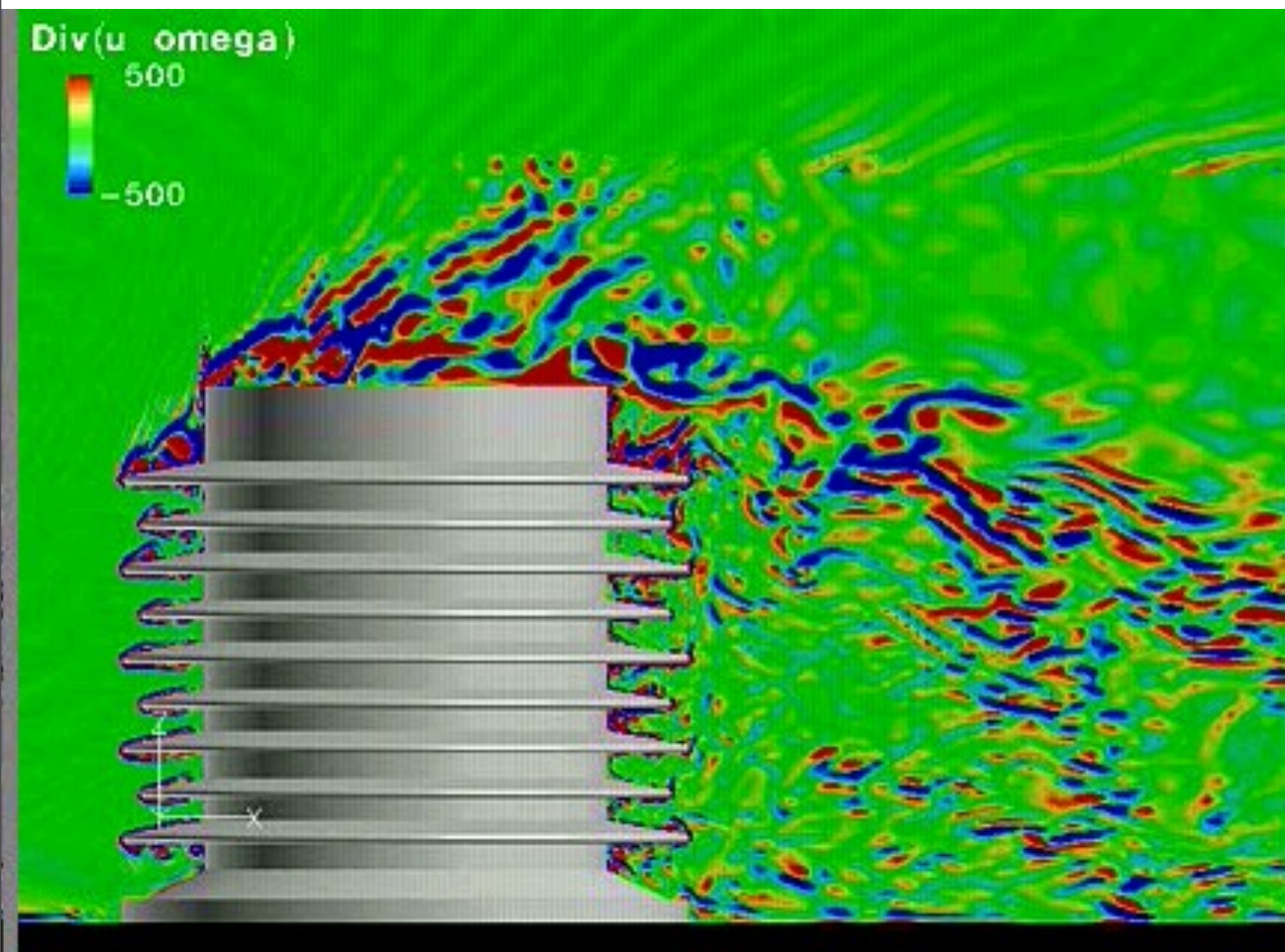
Turbulence & Aeroacoustics



Instantaneous streamwise velocity

Acoustic sources

$\text{Div} \cdot (\mathbf{u} \times \boldsymbol{\omega})$



Methods of analysis

- ⌚ Probability
- ⌚ Dimensional analysis
- ⌚ Asymptotic invariance
- ⌚ Local invariance

- ⌚ Statistical mechanics
- ⌚ Geometry and Topology

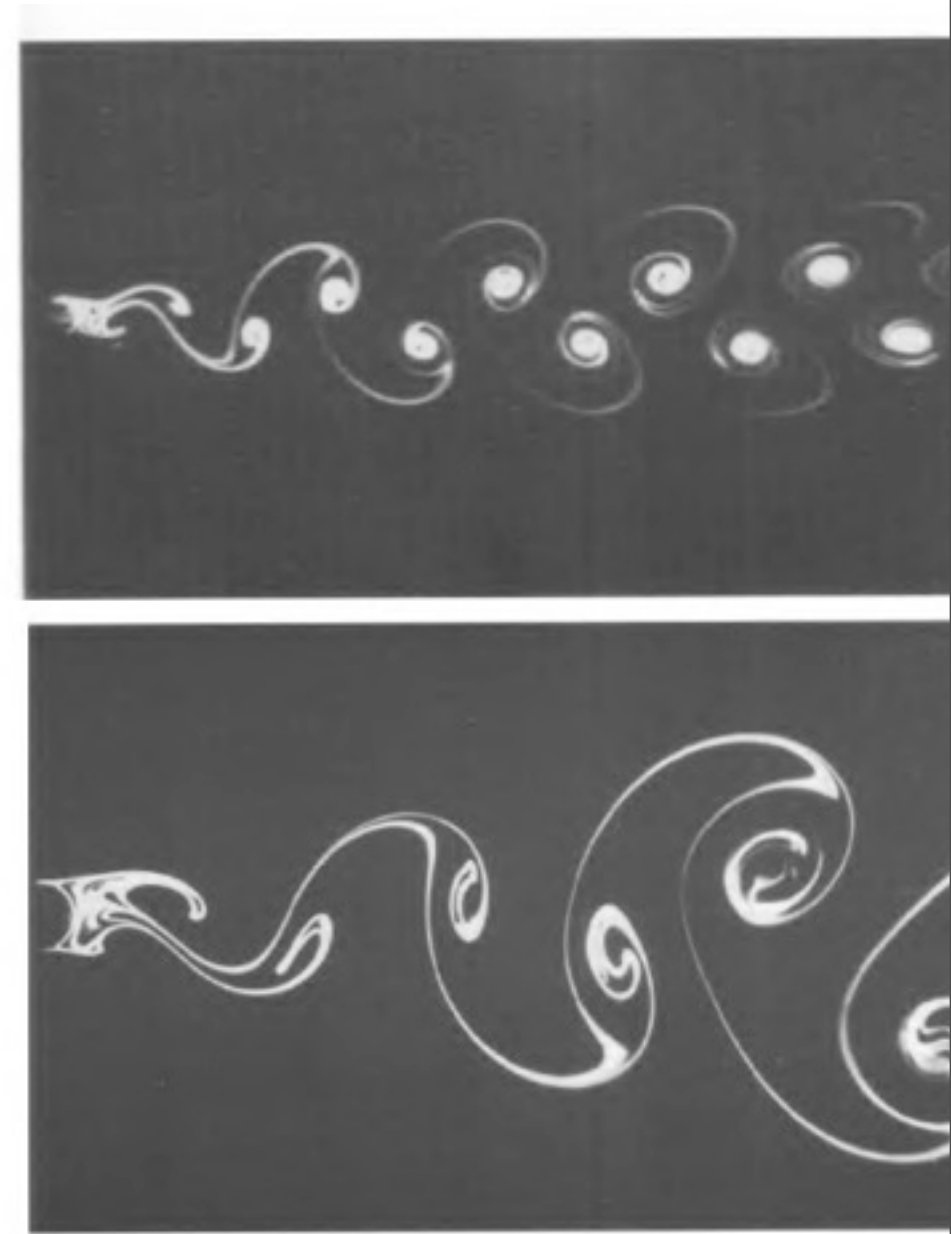
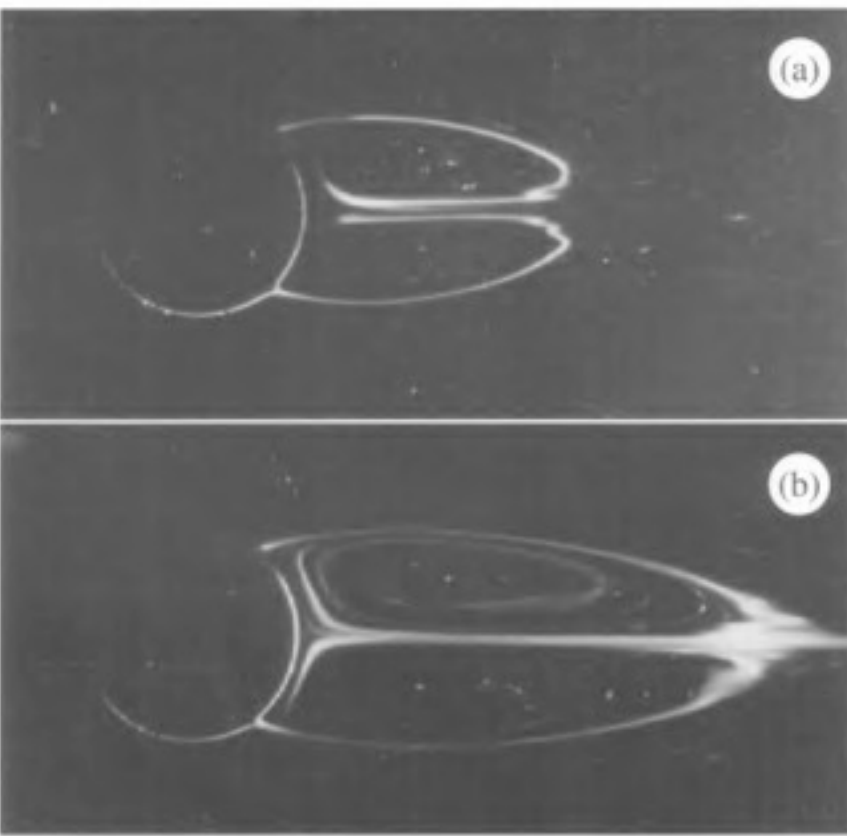
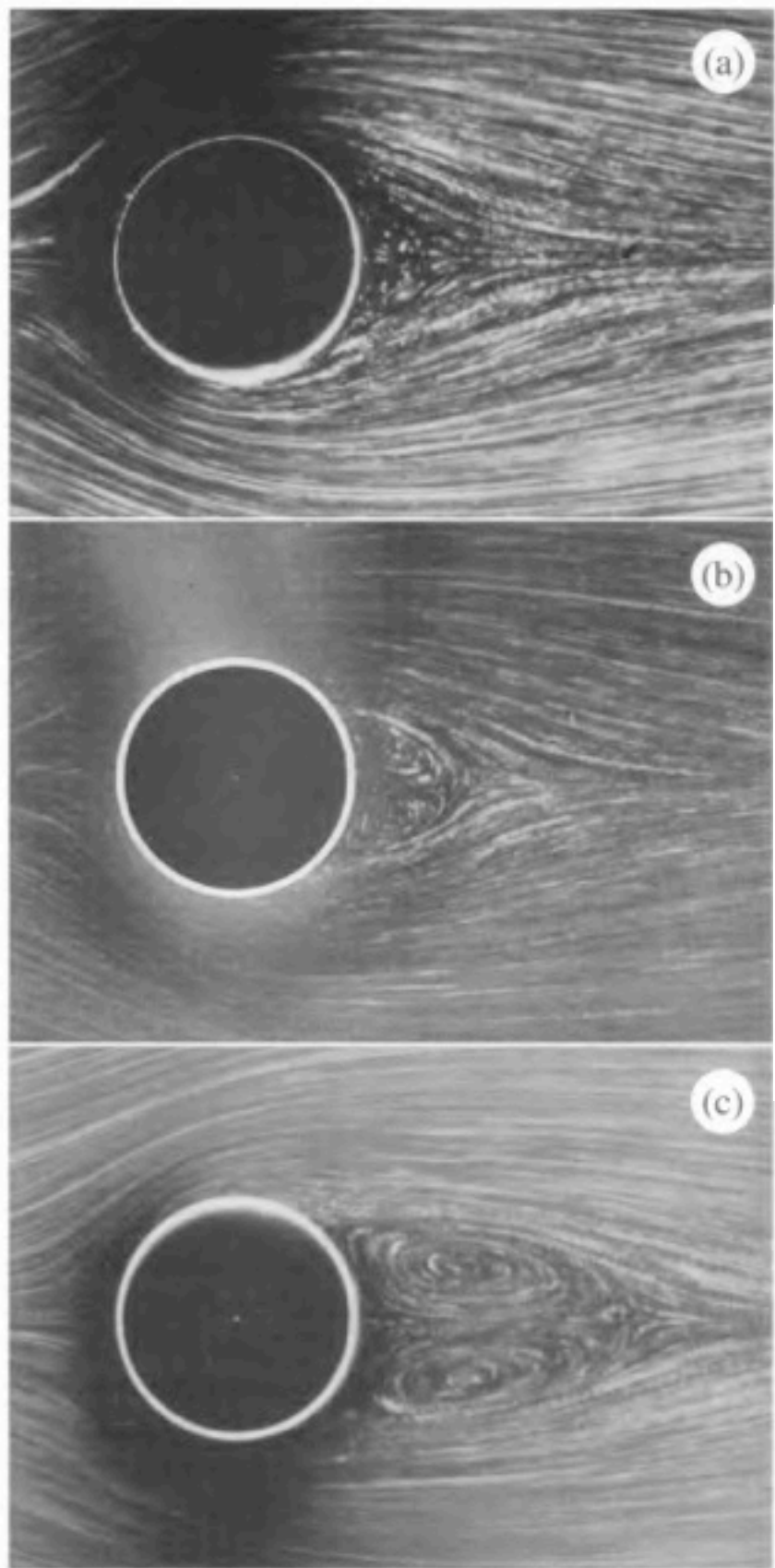
What is a turbulent flow ?

- 🌀 No rigorous definition of **Turbulence** is available
- 🌀 Turbulent flows are flows which exhibit the following features:

1. Three dimensionality
2. Unsteadiness
3. Chaotic
4. Rotational
5. Dissipative
6. Highly diffusive (high mixing property)
7. Multi-scale (Broadband energy spectrum)

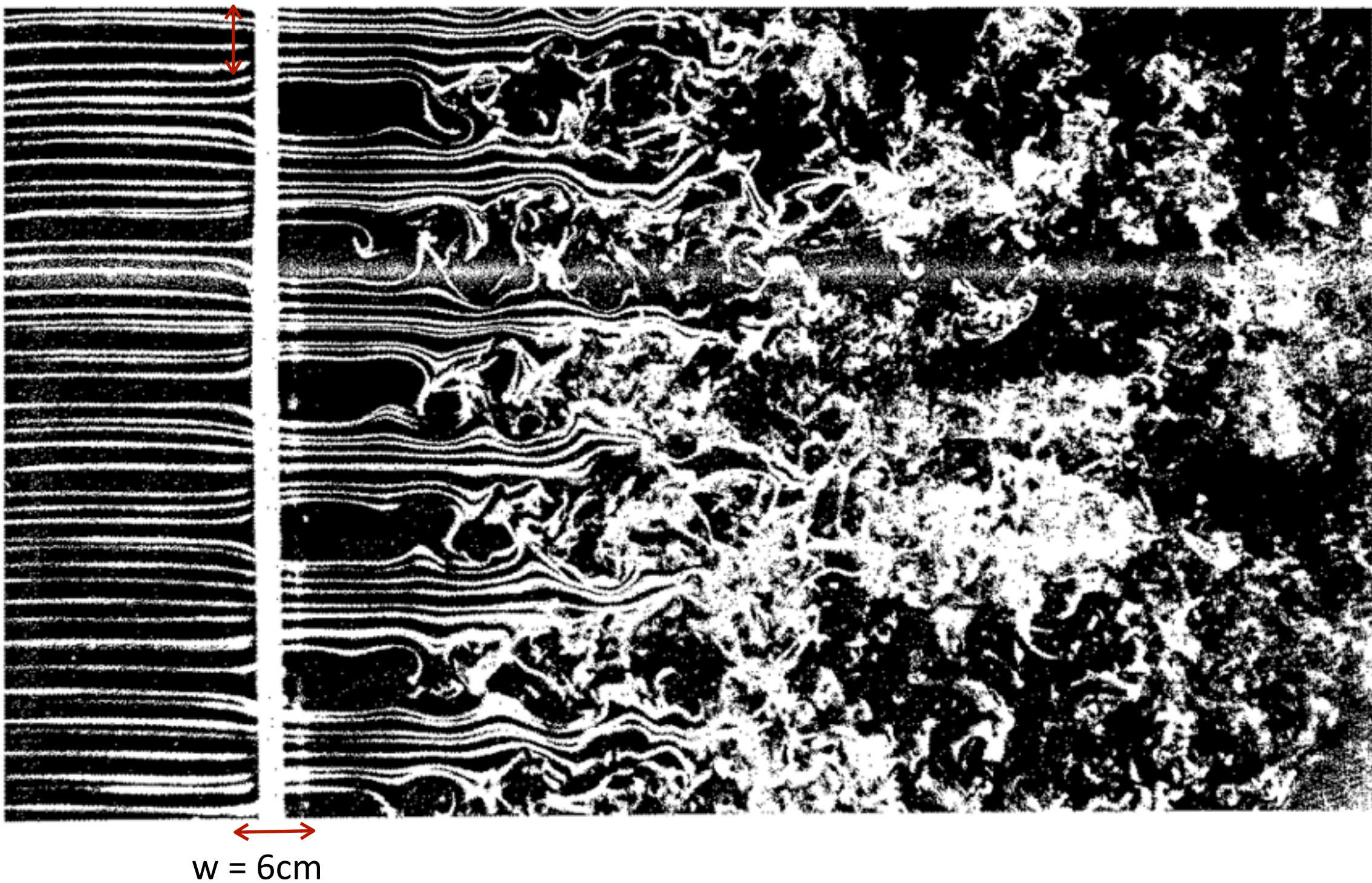
A survey of critical experiments

Transition to turbulence and symmetries



Grid Turbulence

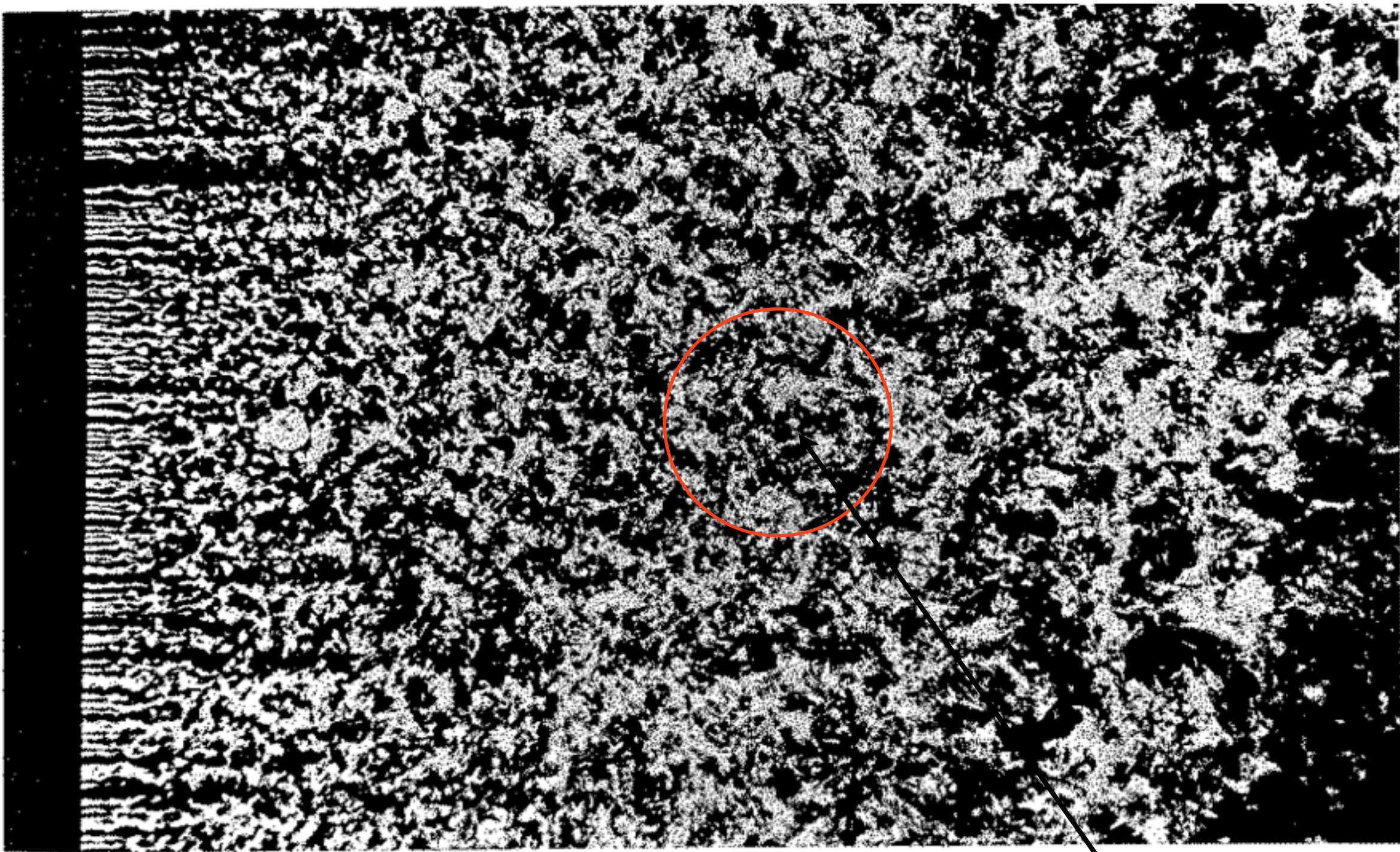
$h = 1/6 \text{ cm};$



Re=1500

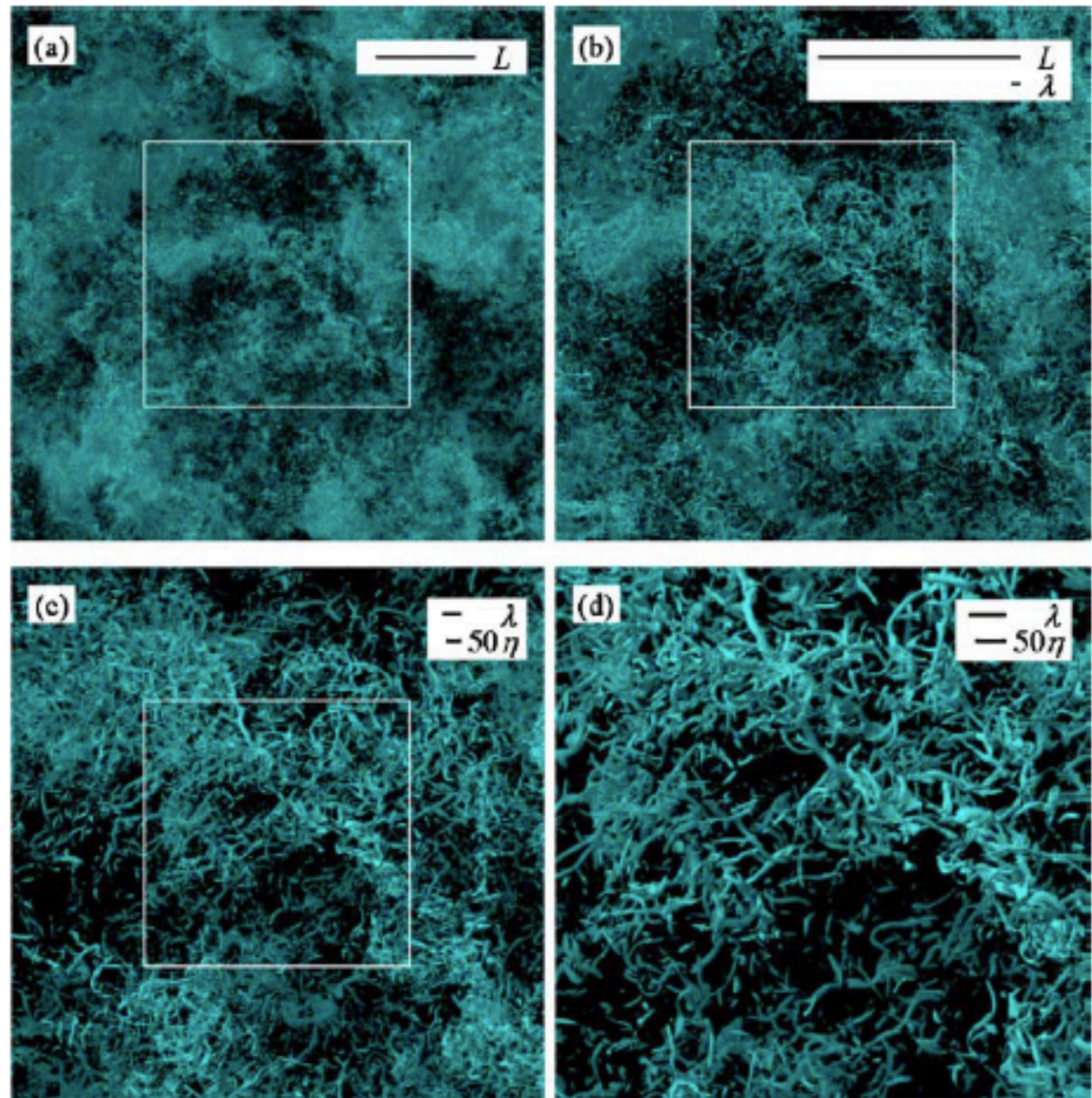
(Van Dyke, Album of fluid motion 1982)

Grid Turbulence: homogeneous



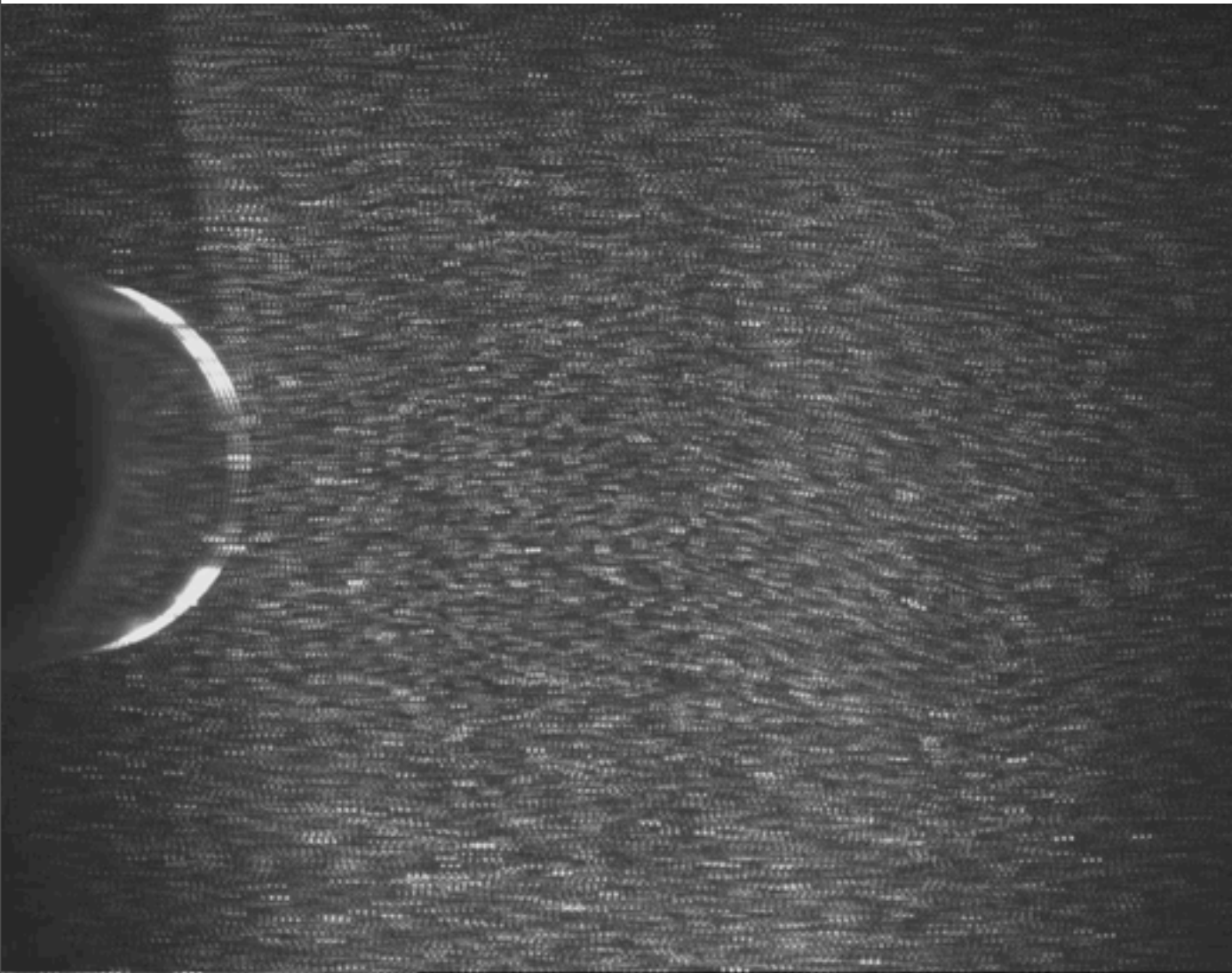
Isotropic

Self-similarity



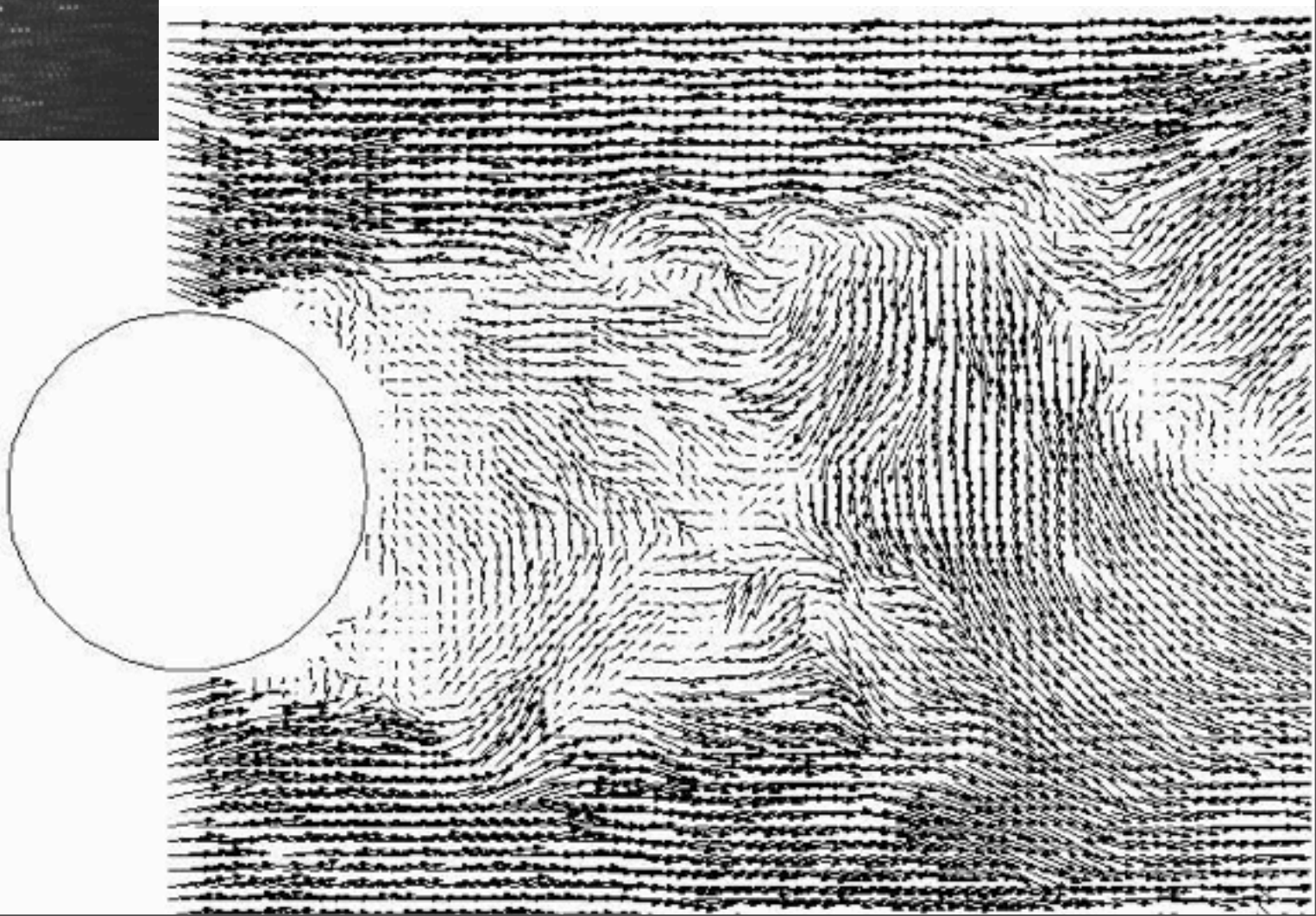
Kaneda & Ishihara
JOT 2006

Figure 3. Intense-vorticity isosurfaces showing the region where $\omega > \langle \omega \rangle + 4\sigma_\omega$. $R_\lambda = 732$. (a) The size of the display domain is $(5984^2 \times 1496) \eta^3$, periodic in the vertical and horizontal directions. (b) Close-up view of the central region of (a) bounded by the white rectangular line; the size of display domain is $(2992^2 \times 1496) \eta^3$. (c) Close-up view of the central region of (b); $1496^3 \eta^3$ (d) Close-up view of the central region of (c); $(748^2 \times 1496) \eta^3$.



PIV

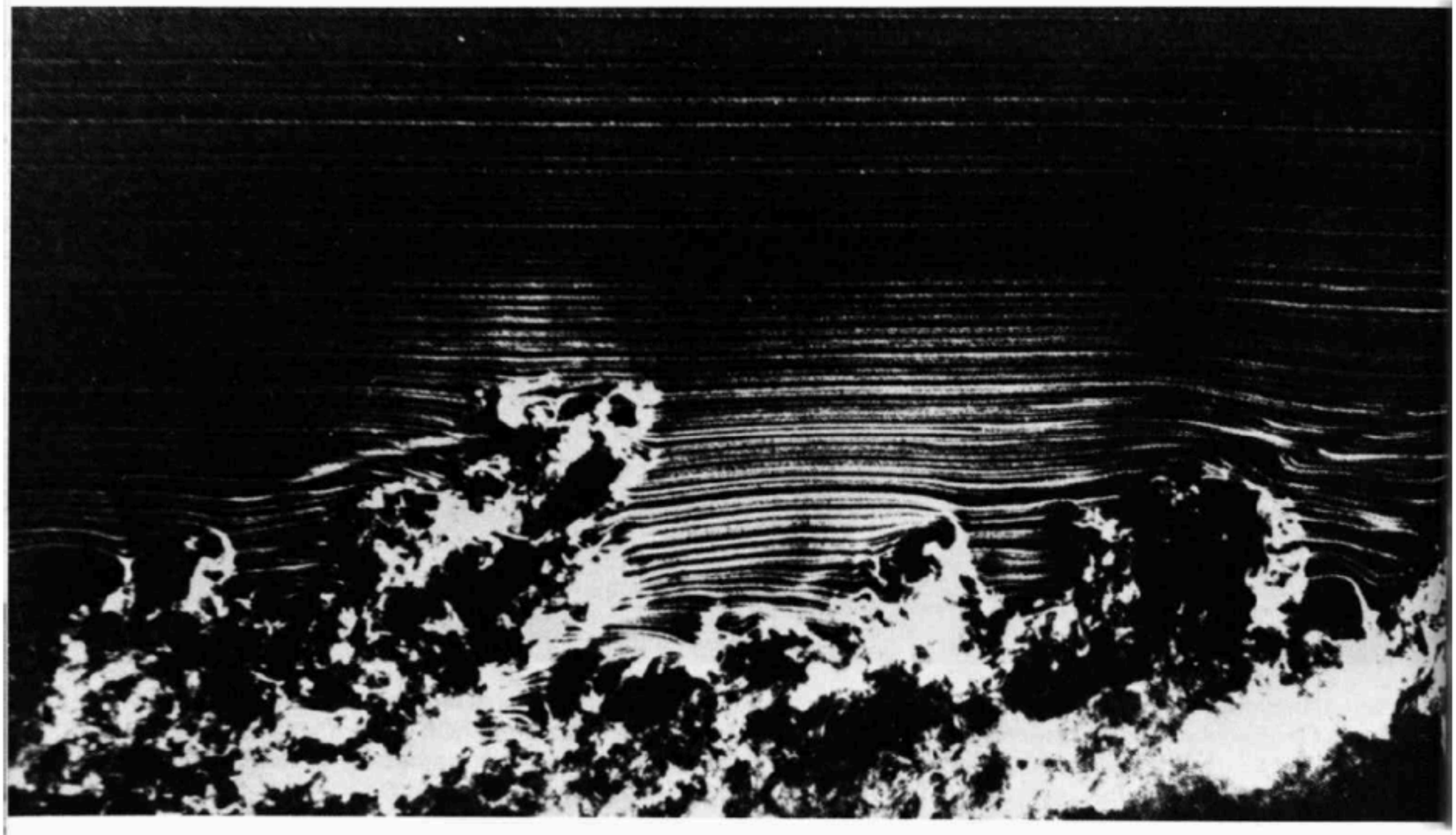
Wake-flow



Turbulent boundary layer

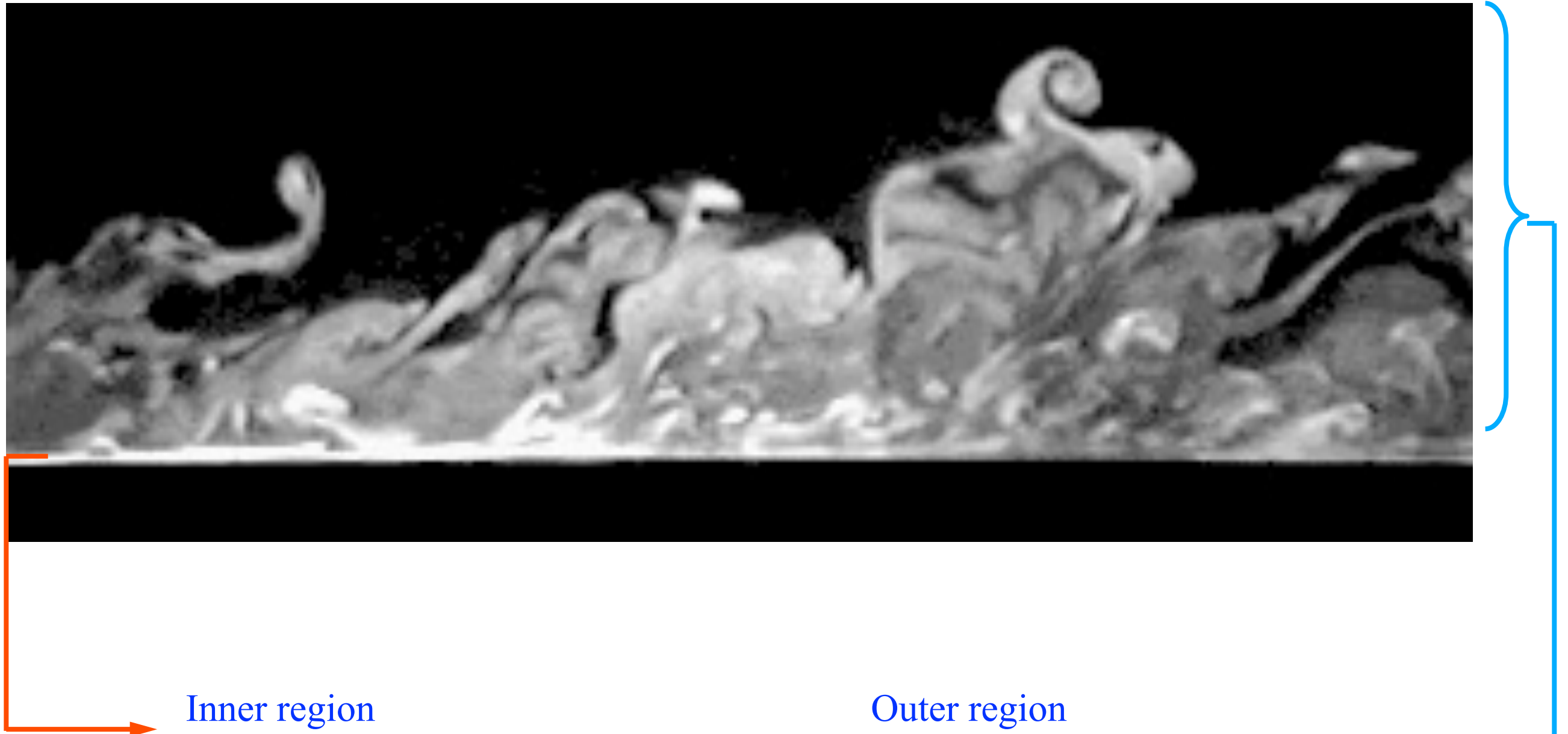
Re=3500

Intermittency



3,3m

Wall-bounded flows: the 2-scale problem



Inner region

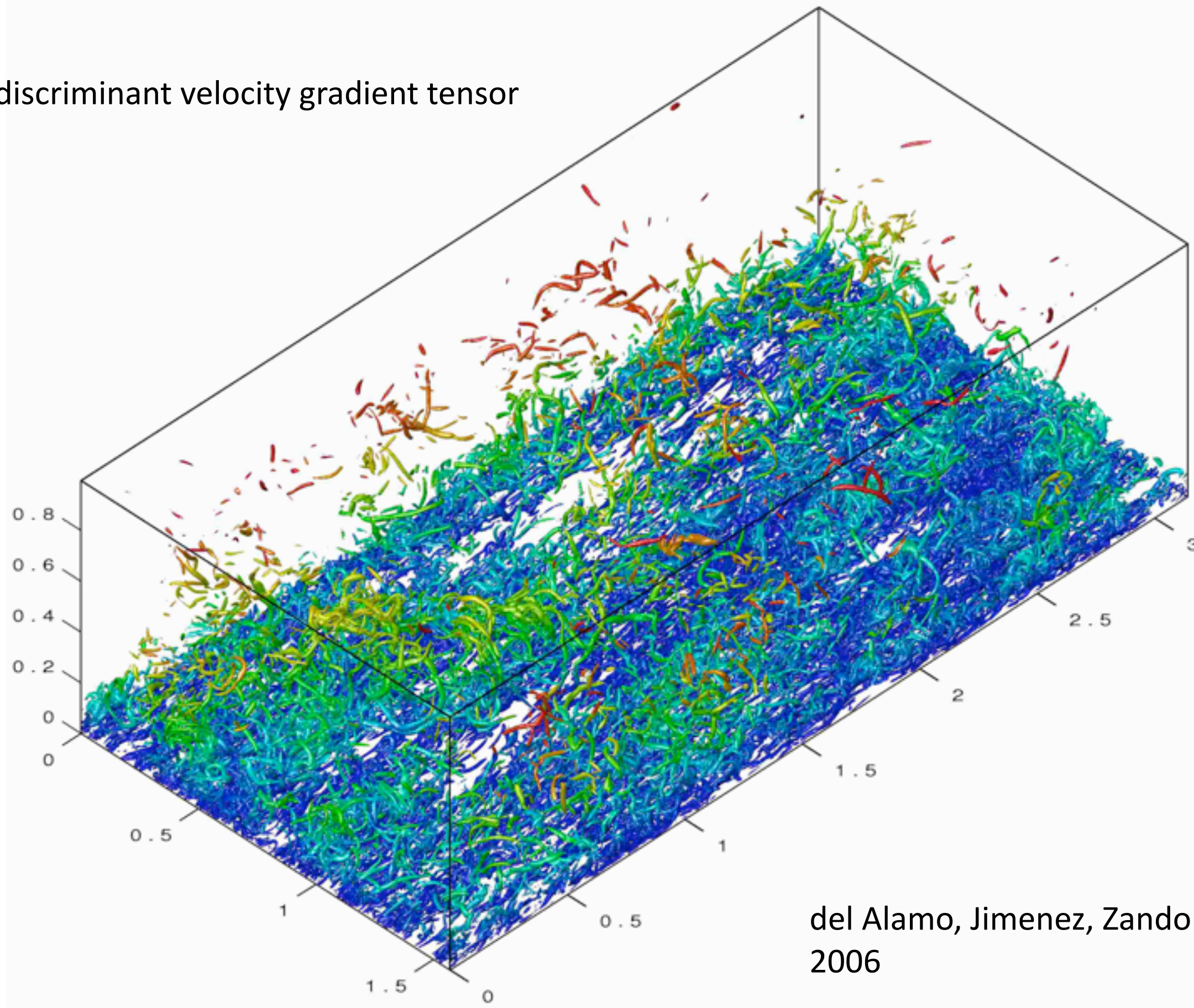
- Production
- Dissipation
- Structures: streaks

Outer region

- Dissipation
- Structure size $\sim \delta$

Turbulent channel

discriminant velocity gradient tensor

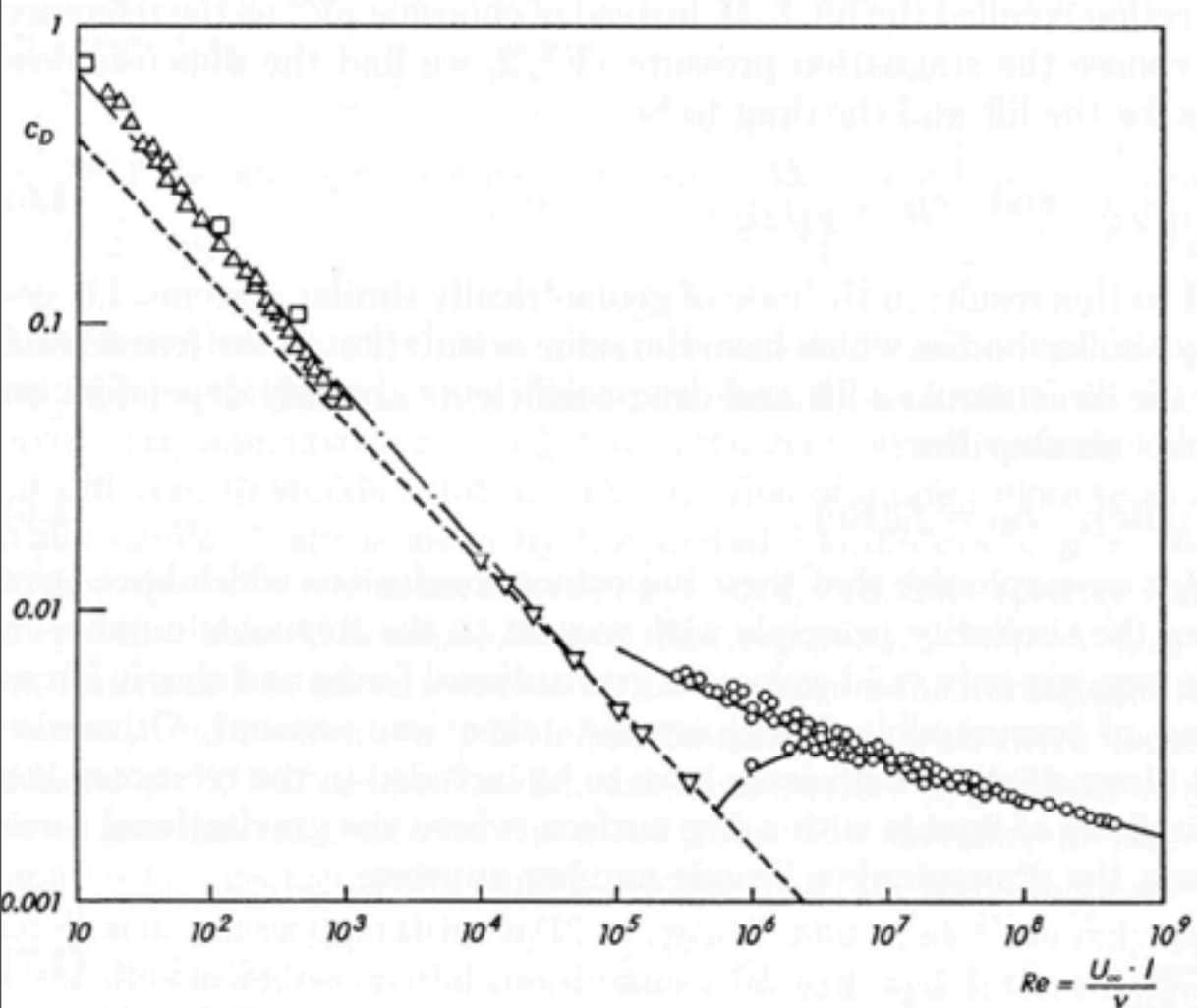


del Alamo, Jimenez, Zandonade, Moser JFM
2006

Drag Coefficient and dissipation

Landau & Lifshitz FM

Plaque plane



Cylindre

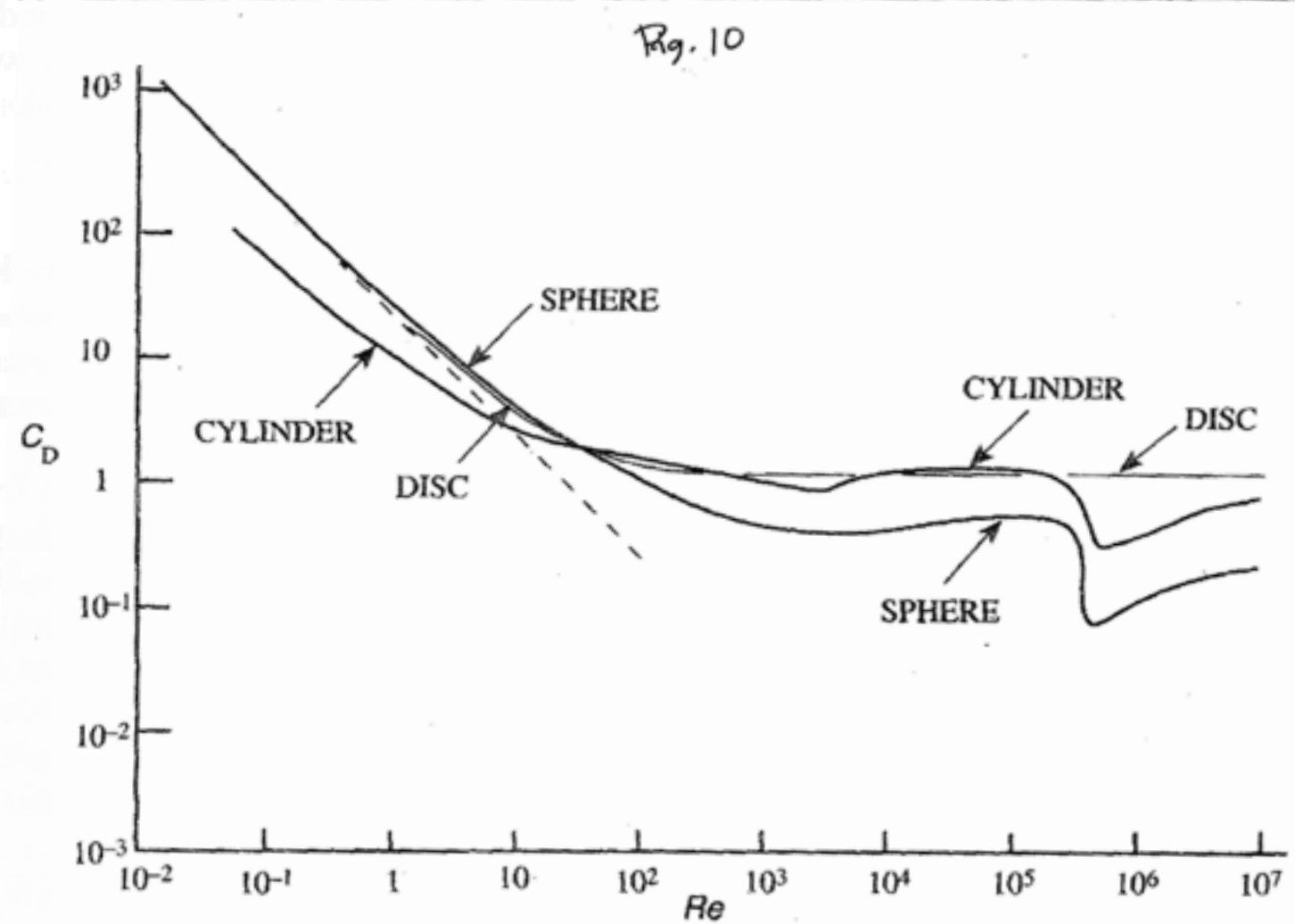


Figure 7.13 Log-log plot of drag coefficient C_D as a function of Reynolds Number Re for spheres, transverse cylinders, and face-on discs. The broken straight line represents Stokes's law.

Boundary layer

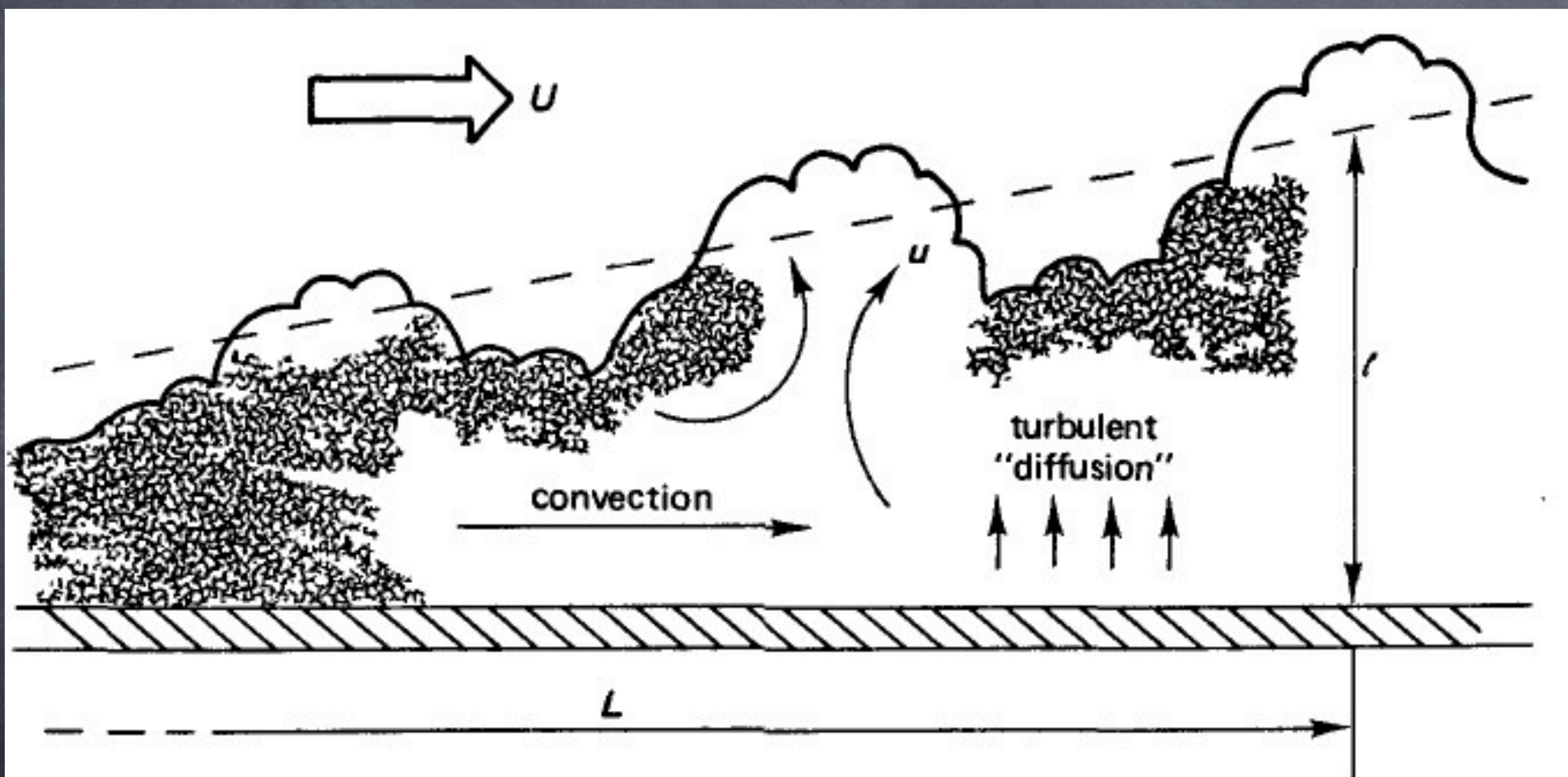
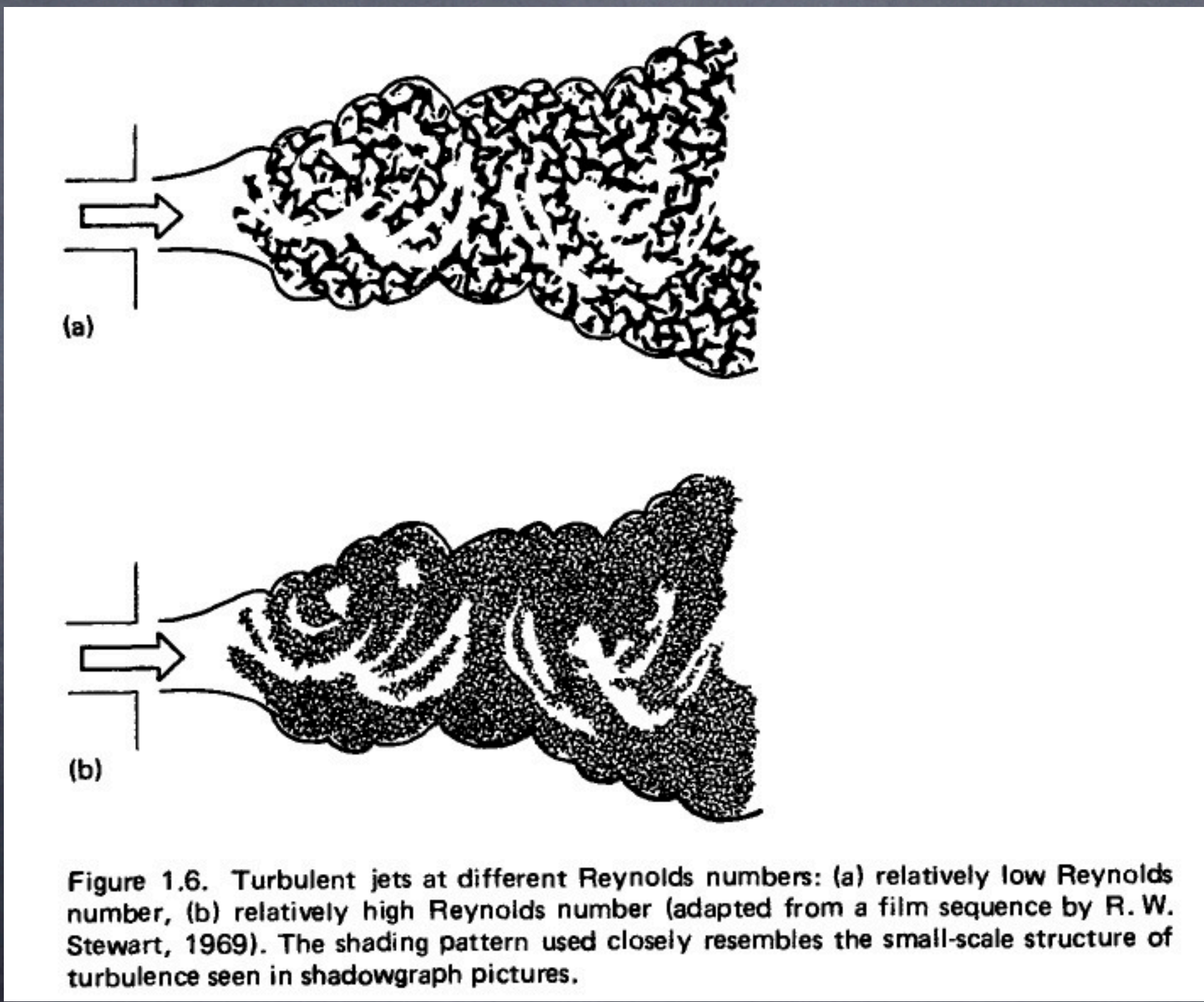


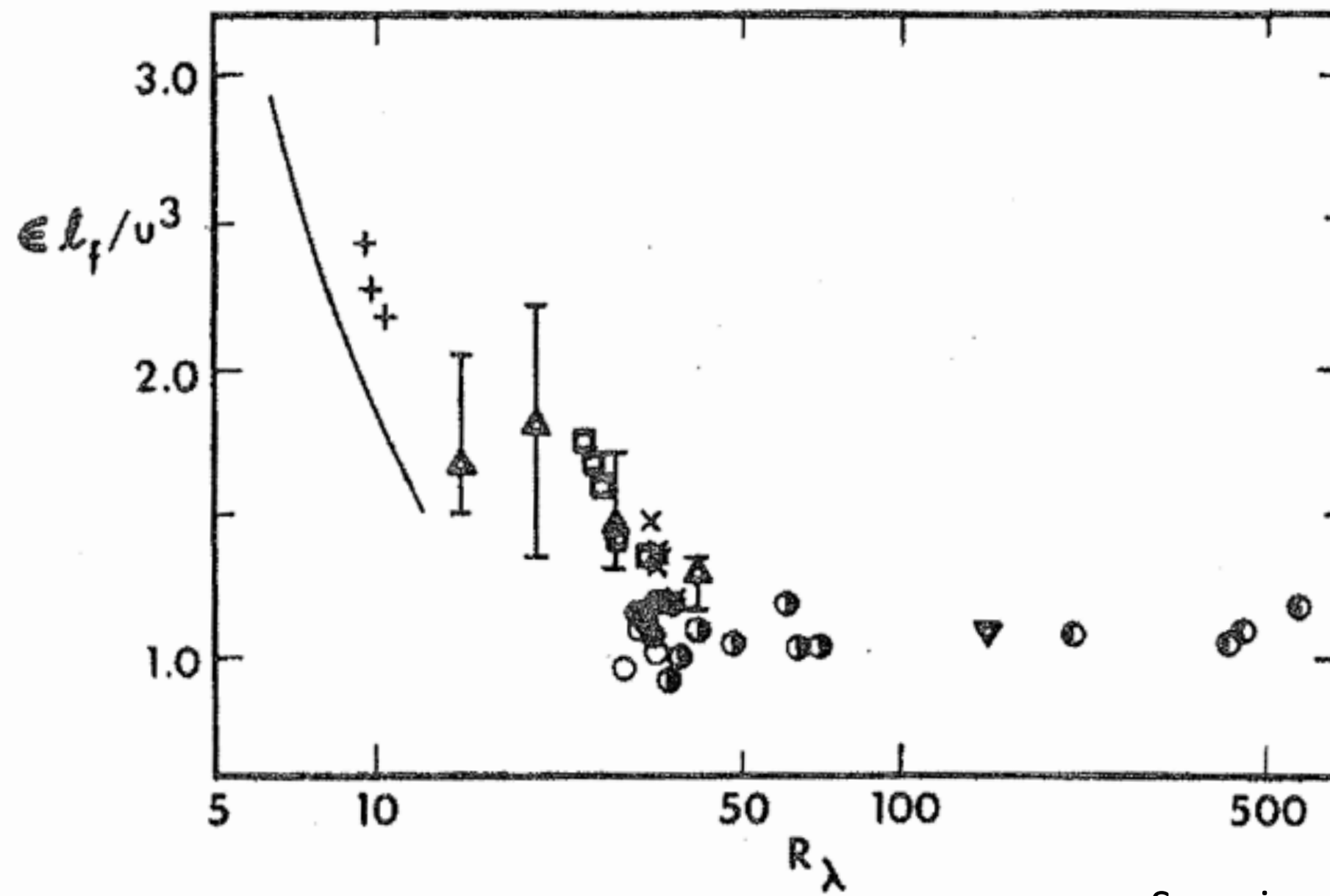
Figure 1.3. Length and velocity scales in a turbulent boundary layer. The time passed since the fluid at L passed the origin of the boundary layer is of order L/U .

Turbulent scales



Zeroth law of Turbulence

GI Taylor 1935



Sreenivasan phys fluids 1984

FIG. 1. The quantity $\epsilon L_f / u^3$ for biplane square-mesh grids. All data except + are for the initial period of delay, and are explained in Table I. + indicate typical data¹³ in the final period of decay. — corresponds to Eq. (1).

Zeroth law of Turbulence

Kaneda et al.

Phys. Fluids, Vol. 15, No. 2, February 2003

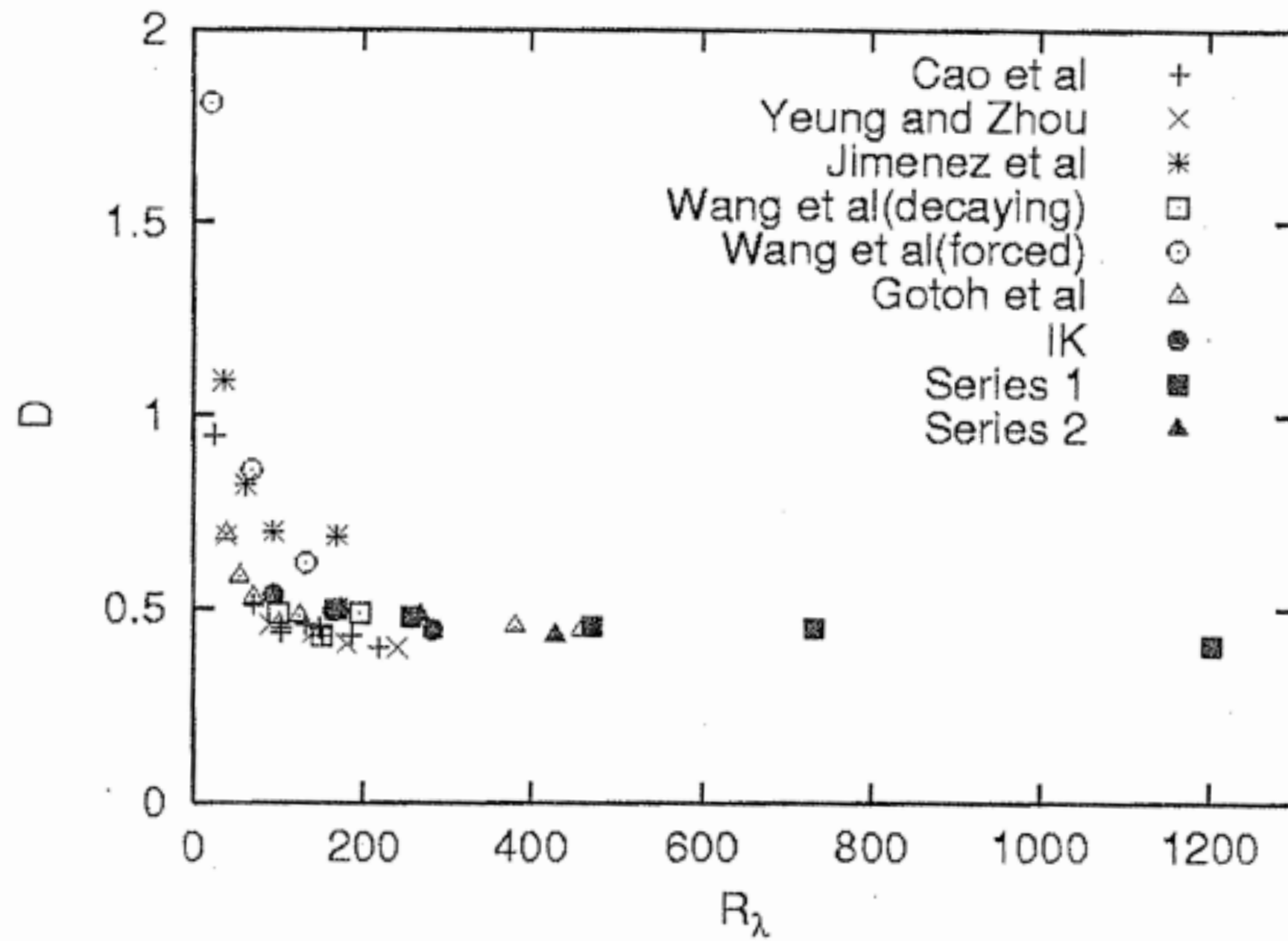
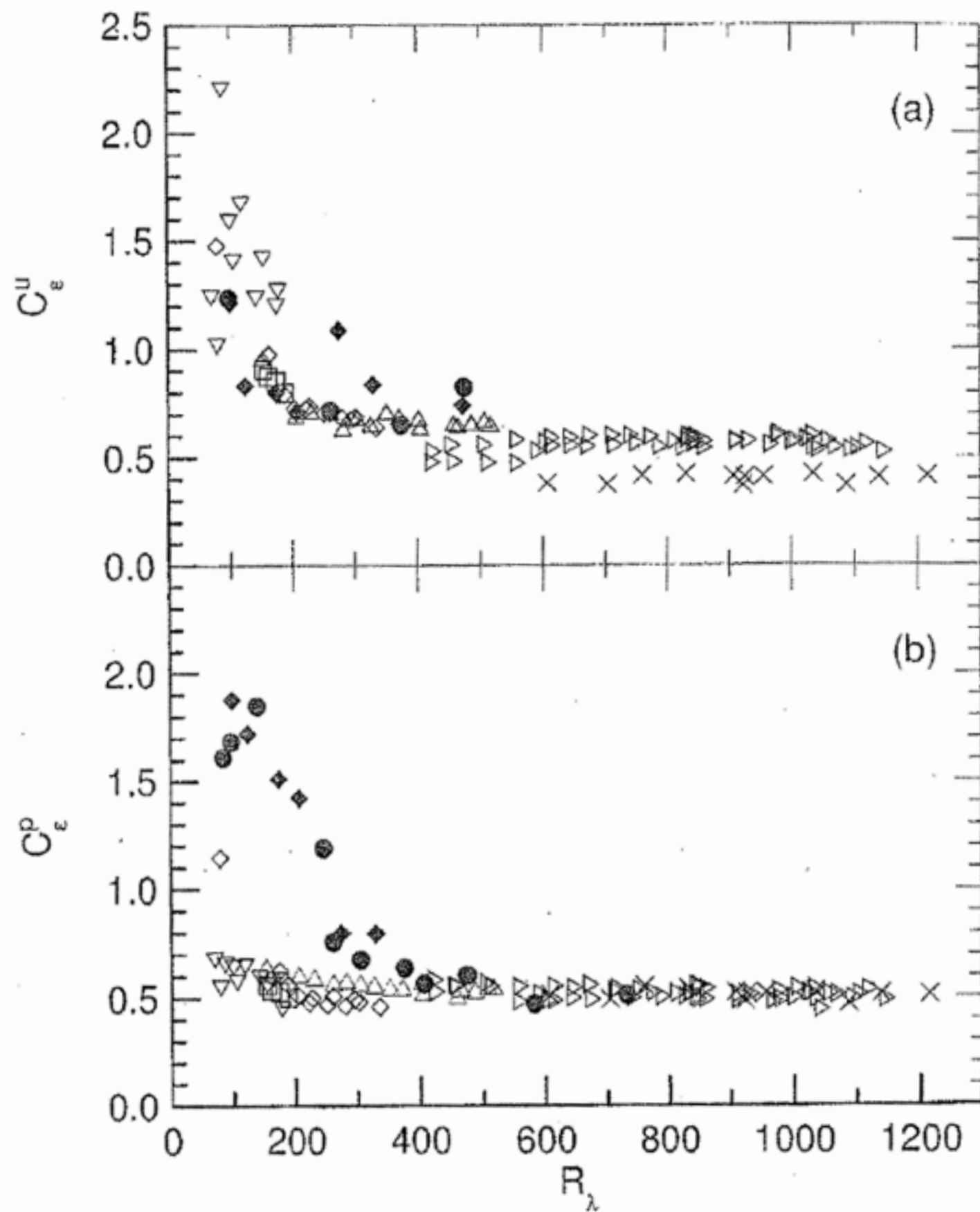


FIG. 3. Normalized energy dissipation rate D versus R_λ from Ref. 5 (data up to $R_\lambda = 250$), Ref. 3 (●, ▲), and the present DNS databases (■, □).

Zeroth law of Turbulence



Pearson et al. Phys Fluids 2002

FIG. 1. Normalized dissipation rate for a number of shear flows. Details as found in this work and Refs. 14–16. a C^{ε} Eq. 3 ; b C^p Eq. 4 . , circular disk, 154 $R = 188$; , pipe, 70 $R = 178$; , normal plate, 79 $R = 335$; , NORMAN grid, 174 $R = 516$; NORMAN grid slight mean shear, $dU/dy = dU/dy_{\max}/2$, 607 $R = 1217$; , NORMAN grid zero mean shear, 425 $R = 1120$; , “active” grid Refs. 14, 15, 100 $R = 731$; , “active” grid, with L_u estimated by Ref. 16. For Ref. 14 data, we estimate $L_p = 0.1$ m and for Ref. 15 data we estimate $L_p = 0.225$ m.

Bounded Flows

Cadot et al. PRE 1997

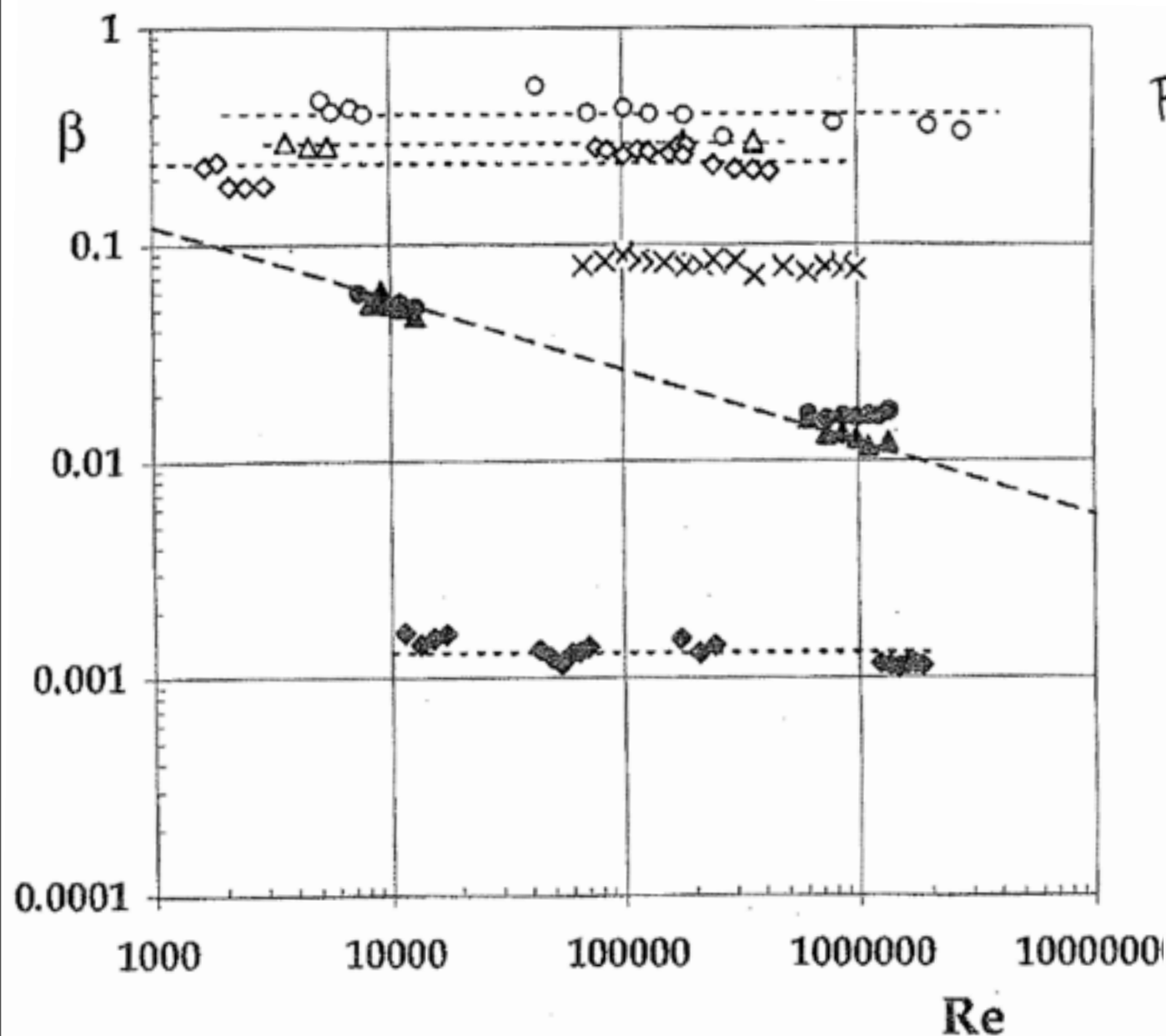


Fig.

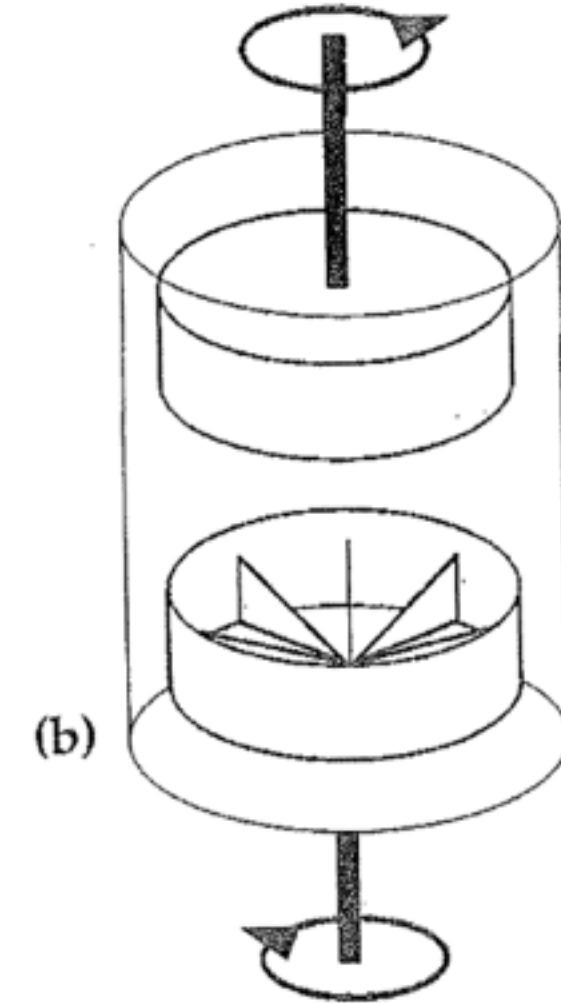
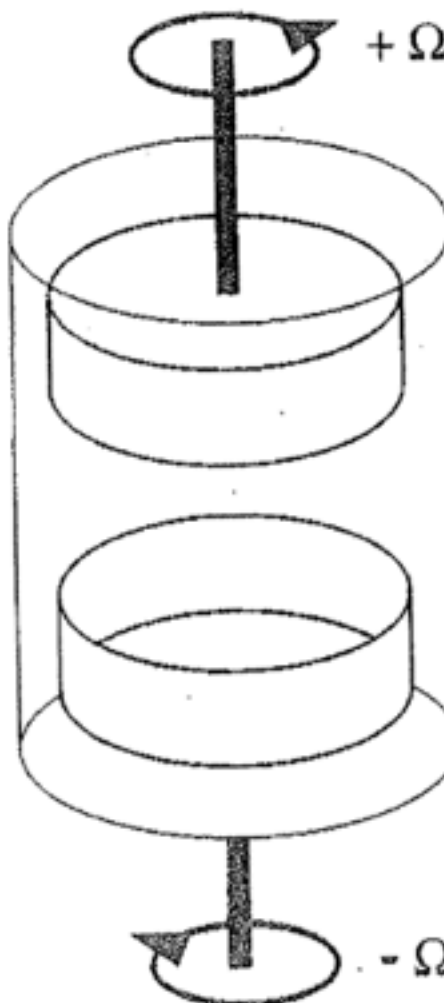
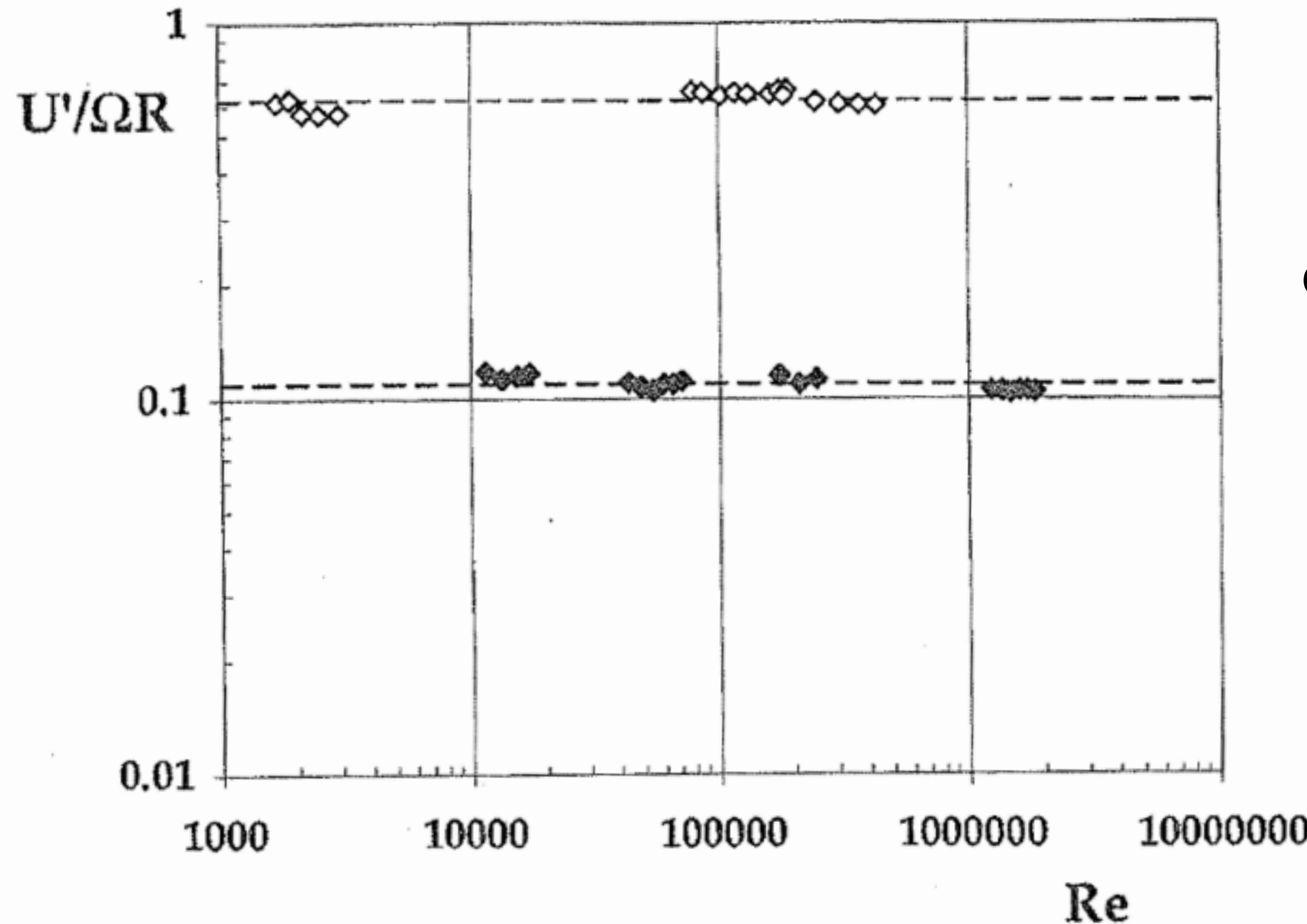


FIG. 2. Experiment A: Logarithmic plots of the nondimensional rate of energy injection β_I and dissipations β_D and β_B as a function of the Reynolds number for the three variants of the experiment. Black symbols: results obtained with smooth stirrers. Triangles (\blacktriangle), rate of energy dissipation β_D ; circles (\bullet), rate of energy injection β_I ; diamonds (\blacklozenge), estimate of the rate of energy β_B dissipated in the bulk of the fluid as estimated from the pressure fluctuations. The dashed line shows a power law dependence proportional to $Re^{-1/4}$. Open symbols: results obtained with the very rough (or inertial) stirrers. Triangles (\triangle), rate of energy dissipation β_D ; circles (\circ), rate of energy injection β_I ; diamonds (\diamond), rate of energy dissipation β_B . Results are obtained with the stirrers having smaller platelets. \times is the mean rate of the energy dissipation β_D .

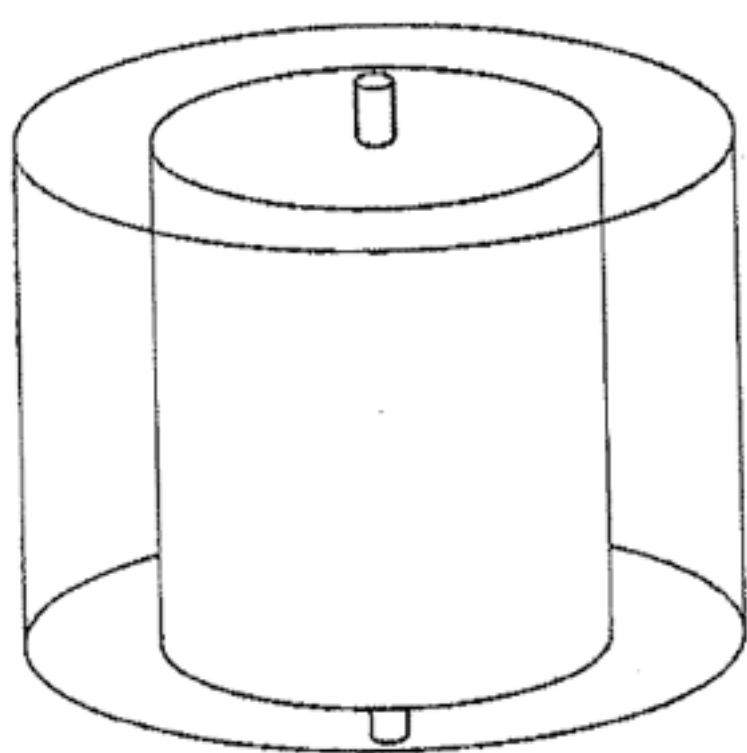
Bounded Flows



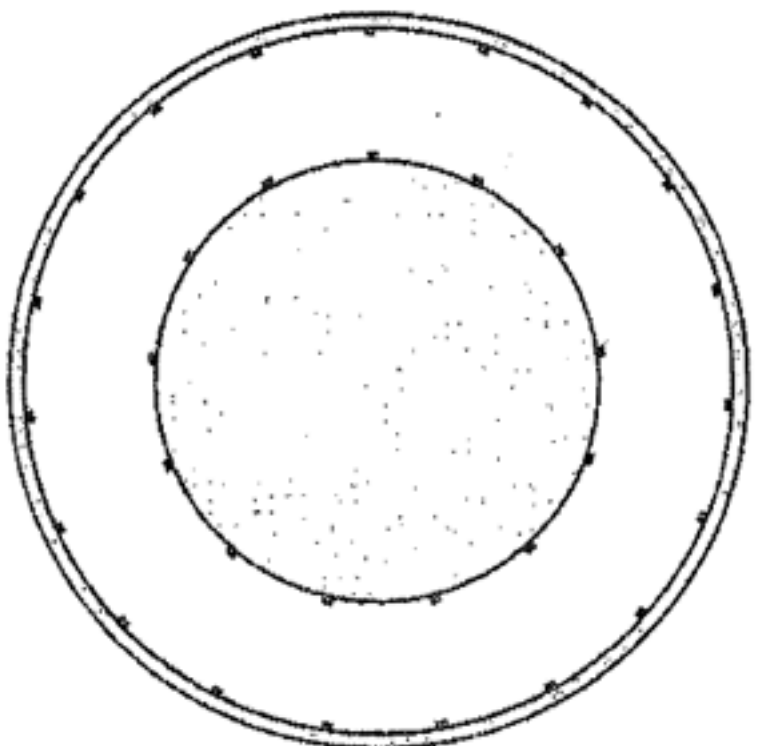
Cadot et al. PRE 1997

FIG. 3. Plot of the typical velocity U' in the bulk of the flow as deduced from the histograms of the pressure fluctuations [see Eq. (7)]. The black triangles (\blacktriangle) are the data obtained with smooth stirrers, and the open ones (\triangle) correspond to the data obtained with the rough ones.

Bounded Flows



a)



Cadot et al. PRE 1997

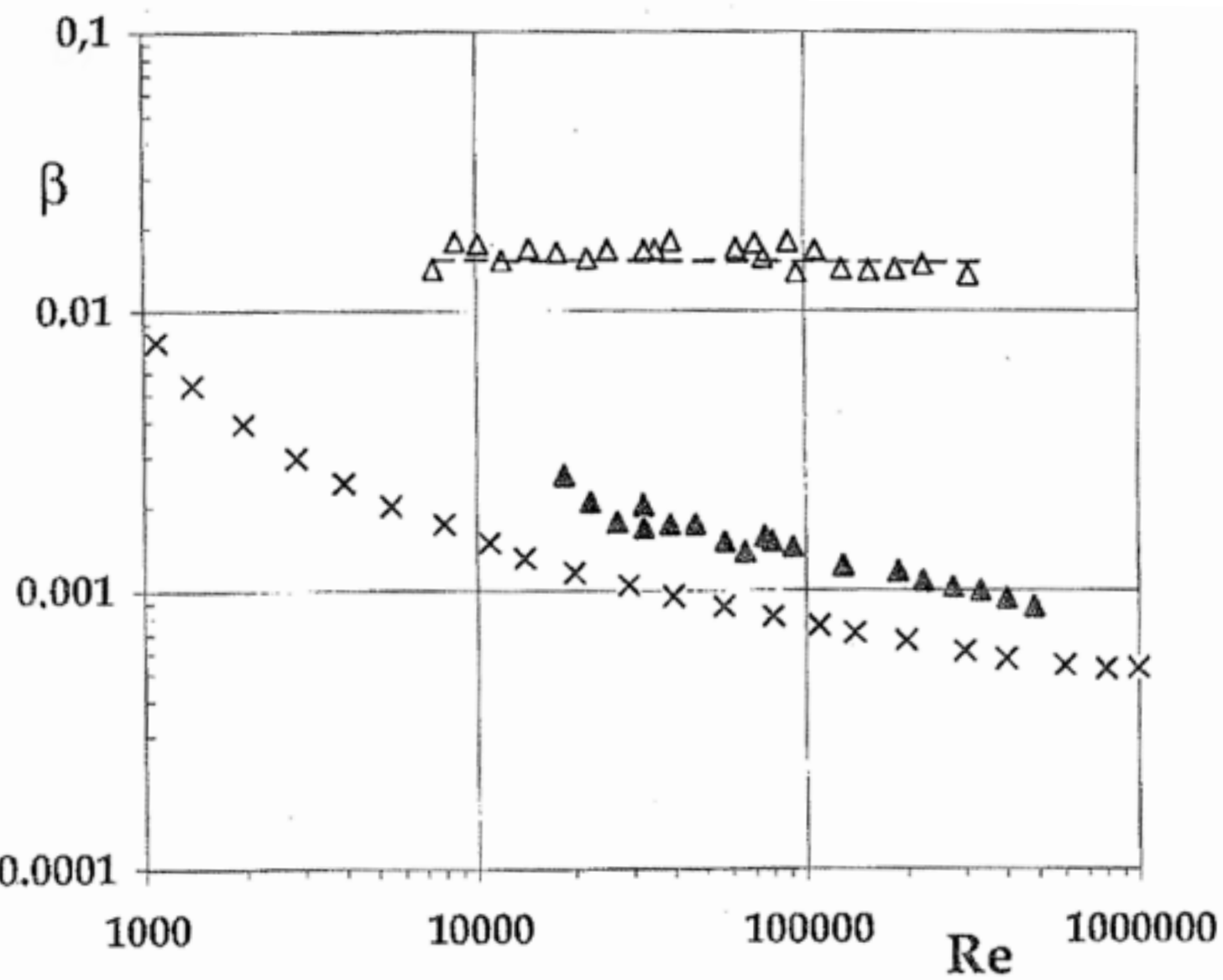


FIG. 5. Couette-Taylor experiments. Logarithmic plots of the nondimensional rates of energy dissipation β_D as a function of the Reynolds number. The black triangles (\blacktriangle) are the results obtained with smooth cylinders, and the open ones (Δ) correspond to those obtained with the ribbed ones. The crosses (\times) show for comparison the rates of energy injection β_D deduced from the data obtained with smooth cylinders by Lathrop, Finenberg, and Swinney [8].

Present physical model

Framework:

- Incompressible flow
- Single phase flow
- Single species flow
- Newtonian flow
- passive scalar for temperature/pollutant modelling
- no coupled dynamical field (magnetic field, density, ...)

Governing equation

$$\rho \left(\frac{\partial}{\partial t} \underline{u} + \underline{\nabla} \cdot (\underline{u} \otimes \underline{u}) \right) = -\underline{\nabla} p + \mu \Delta \underline{u} + \underline{f}$$

$$\underline{\nabla} \cdot \underline{u} = 0$$

$$\rho \left(\frac{\partial}{\partial t} T + \underline{\nabla} \cdot (uT) \right) = \kappa \Delta T$$

Preliminary remarks

Poisson equation for pressure (elliptic equation)

$$-\Delta p = \underline{\nabla} \cdot \underline{\nabla} \cdot (\underline{u} \otimes \underline{u}) - \underline{\nabla} \cdot \underline{f}$$

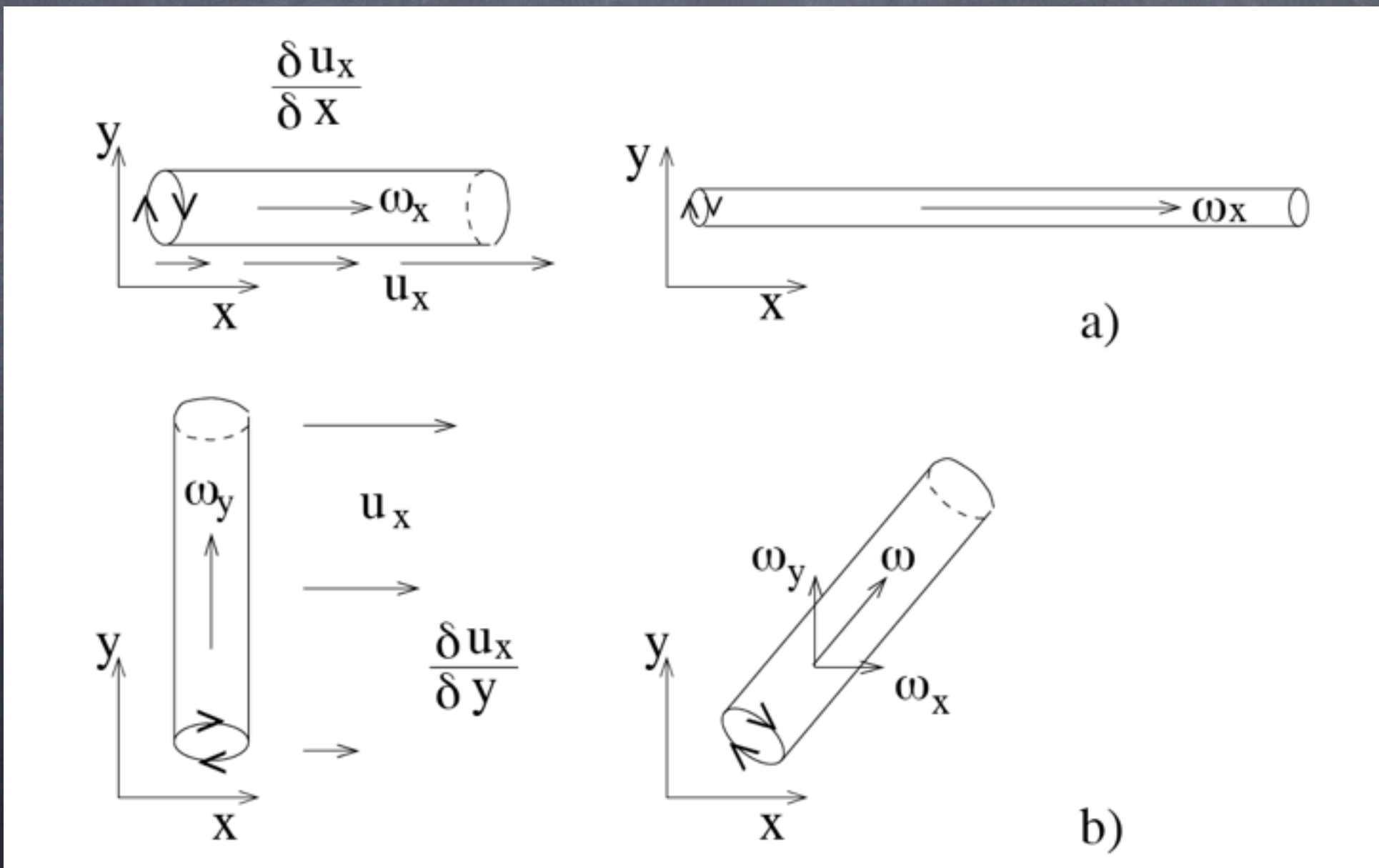
General Green-function-based solution

$$p(\underline{x}, t) = \iiint - [\underline{\nabla} \cdot \underline{\nabla} \cdot (\underline{u} \otimes \underline{u}) + \underline{\nabla} \cdot \underline{f}] (\underline{y}, t) \mathcal{G}(\underline{x}, \underline{y}) d\underline{y}$$

Consequences:

physical inconsistency in the acoustic limit
pressure = enslaved Lagrangian, not independent physical variable

vortex stretching



Equation simmetry

